QUANTUM FLUCTUATIONS AND TRANSPORT IN MESOSCOPIC PHYSICS

Teemu Ojanen

Dissertation for the degree of Doctor of Science in Technology to be presented with due permission of the Department of Engineering Physics and Mathematics for public examination and debate in Auditorium F1 at Helsinki University of Technology (Espoo, Finland) on the 30^{th} of November, 2007, at 12 o'clock noon.

Helsinki University of Technology
Department of Engineering Physics and Mathematics
Low Temperature Laboratory

Teknillinen korkeakoulu
Teknillisen fysiikan ja matematiikan osasto
Kylmälaboratorio

ABSTRACT OF DOCTORAL DISSERTATION	HELSINKI UNIVERSITY OF TECHNOLOGY P. O. BOX 1000, FI-02015 TKK http://www.tkk.fi

Author Teemu Ojanen

Name of the dissertation

Quantum fluctuations and transport in mesoscopic physics

Manuscript submitted 20.8.2007	Manuscript revised 30.10.2007
Date of the defence 30.11.2007	
☐ Monograph	☒ Article dissertation (summary + original articles)

Department	Department of Engineering Physics and Mathematics
Laboratory	Low Temperature Laboratory
Field of research	Theoretical condensed matter physics
Opponent(s)	Prof. Frank Wilhelm
Supervisor	Acad. Prof. Risto Nieminen
Instructor	Dr. Tero Heikkilä

Abstract

Mesoscopic physics and nanoelectronics concentrate on systems with dimensions somewhere between atomic and everyday macroscopic scale. Modern technology enables construction of submicron nanostructures where modeling based on classical physics has proven inadequate. It is possible to design electric circuits where dynamics of single electrons and photons are controlled using state-of-the-art experimental methods. For quantitative understanding of these systems it is necessary to resort to a quantum-mechanical description. Quantum phenomena, such as tunneling and a wave-like interference of particles, are essential ingredients of physics in mesoscopic systems. Field of mesoscopic physics contains a rich variety of topics ranging from fundamental condensed matter physics to quantum information processing and possible future technological applications.

This thesis presents theoretical studies of mesoscopic quantum phenomena in nanostructures and small electronic devices. We have focused on effects of environment fluctuations and investigated connections between fluctuations and transport phenomena. Decoherence in quantum bits (qubits) and quantum state engineering in superconducting circuits are also studied. The theoretical analysis in each case requires an open-system treatment.

Effects of current fluctuations on quantum probe systems have been studied in detail. We have calculated transitions induced by current noise and discussed how these could be used for characterization of fluctuations. We have also shown that electric fluctuations play a key role in radiation and photon heat transport in nanostructures. Motivated by recent advances in mesoscopic electron-photon systems, we have studied a response of a coupled resonator-qubit system, squeezing of quantum fluctuations in small superconducting circuits and investigated decoherence in Josephson flux qubits.

Keywords mesoscopic quantum phenomena, decoherence and noise, quantum transport	
ISBN (printed) 978-951-22-9052-9	ISSN (printed)
ISBN (pdf) 978-951-22-9053-6	ISSN (pdf)
Language English	Number of pages 46
Publisher Multiprint Oy	
Print distribution Low Temperature Laboratory, TKK	
☒ The dissertation can be read at http://lib.tkk.fi/Diss/	

VÄITÖSKIRJAN TIIVISTELMÄ	TEKNILLINEN KORKEAKOULU PL 1000, 02015 TKK http://www.tkk.fi

Tekijä Teemu Ojanen

Väitöskirjan nimi

Kvanttifluktuaatiot ja kuljetusilmiöt mesoskooppisissa rakenteissa

Käsikirjoituksen päivämäärä 20.8.2007	Korjatun käsikirjoituksen päivämäärä 30.10.2007
Väitöstilaisuuden ajankohta 30.11.2007	
☐ Monografia	☒ Yhdistelmäväitöskirja (yhteenveto + erillisartikkelit)

Osasto	Teknillisen fysiikan ja matematiikan osasto
Laboratorio	Kylmälaboratorio
Tutkimusala	Teoreettinen kondensoituneen aineen fysiikka
Vastaväittäjä(t)	prof. Frank Wilhelm
Työn valvoja	akat. prof. Risto Nieminen
Työn ohjaaja	dos. Tero Heikkilä

Tiivistelmä

Mesoskooppisessa fysiikassa ja nanoelektroniikassa tutkitaan rakenteita joiden kokoluokka on jossakin atomaaristen ja arkipäiväisten mittojen välimaastossa. Modernin teknologian avulla on mahdollista tuottaa alle mikrometrin kokoisia nanorakenteita, joiden mallintamisessa klassisen fysiikan lait ovat osoittautuneet riittämättömiksi. Uusimpien kokeellisten menetelmien avulla on mahdollista kontrolloida yksittäisten elektronien ja fotonien dynamiikkaa, jolloin systeemien teoreettinen mallintaminen edellyttää ilmiöiden kvanttimekaanista kuvaamista. Kvantti-ilmiöillä, kuten tunneloituminen ja hiukkasten aaltomainen interferenssi, on keskeinen asema mesoskooppisissa rakenteissa. Mesoskooppinen fysiikka kattaa laajan aihevalikoiman perusfysiikan ilmiöistä aina kvantti-informaatioteoriaan ja tulevaisuuden teknologisiin sovelluksiin.

Väitöskirja koostuu mesoskooppisten kvantti-ilmiöiden ja nanoelektroniikan teoreettisesta tutkimuksesta. Erityisesti käsitellään ympäristön fluktuaatioiden vaikutusta nanoskaalan kvanttisysteemeihin ja selvitetään fluktuaatioiden yhteyksiä kuljetusteoriaan. Lisäksi tutkitaan dekoherenssia kvanttibiteissä ja kvanttievoluution kontrollointia suprajohtavissa virtapiireissä. Teoreettinen käsittely nojaa avoimien kvanttisysteemien formalismeihin.

Epätasapainofluktuaatioiden aiheuttamia ympäristöilmiöitä käsitellään yleisten kvanttidetektorisysteemien tapauksessa. Virtafluktuaatioiden luonnetta karakterisoidaan tutkimalla sen indusoimia transitioita detektorisysteemissä. Virtafluktuaatiot liittyvät läheisesti myös säteilyyyn ja fotonilämmönkuljetukseen nanorakenteissa. Viimeaikaisten mesosokooppisiin elektroni-fotonistruktuureihin liittyvien kokeellisten läpimurtojen motivoimana tutkitaan kytketyn resonaattorin ja kvanttibitin dynaamista vastetta, kvanttifluktuaatioiden manipulointia suprajohtavissa piireissä ja aaltojohteissa sekä suprajohtavien vuokvanttibittien dekoherenssia soveltaen uusimpien mikroaaltomenetelmien ideoita.

Asiasanat Mesoskooppiset kvantti-ilmiöt, dekoherenssi ja kohina, kuljetusilmiöt

ISBN (painettu) 978-951-22-9052-9	ISSN (painettu)
ISBN (pdf) 978-951-22-9053-6	ISSN (pdf)
Kieli englanti	Sivumäärä 46

Julkaisija Multiprint Oy

Painetun väitöskirjan jakelu Kylmälaboratorio, TKK

☒ Luettavissa verkossa osoitteessa http://lib.tkk.fi/Diss/

Preface

This Thesis was initiated in late 2003 when I joined Low Temperature Laboratory in Helsinki University of Technology. Low Temperature Laboratory has a prestigious tradition of scientific research and has maintained its status as a high-profile research center for decades. I would like to thank the head of the laboratory Prof. Mikko Paalanen for his immediate decision to employ me as a doctoral student after our first discussion regarding the subject. It has always been easy and relaxed to communicate with him. I thank my instructor Dr. Tero Heikkiä for his many efforts to work in my favor in big and small issues during my time in LTL and for his scientific influence on my thesis work. Academy professor Risto Nieminen is thanked for acting as a supervisor and for arranging practical affairs concerning my dissertation. I would like to express my gratitude to my collaborators Antti Niskanen, Janne Salo, Ville Bergholm, Mikko Möttönen, Olli-Pentti Saira, Yasunobu Nakamura and Abdufarrukh Abdumalikov. Professors Jukka Pekola and Pertti Hakonen are acknowledged for scientific inspiration and many fruitful discussions.

I have been privileged to work in an inspiring, interesting and challenging environment provided by LTL. My past and present co-workers are thanked for creating the great atmosphere that I have enjoyed all these years. In this context I have to mention René Lindell, Tommi Nieminen, Mika Sillanpää, Jouni Flyktman, Juha Vartiainen, Teijo Lehtinen, Jani Kivioja, Pauli Virtanen, Matti Laakso, Juha Voutilainen, Antti Puska, Matti Tomi, Antti Paila, Risto Hänninen, Lorenz Lechner, David Gunnarsson and Rob Blaauwgeers. Besides those mentioned above, I have made many friends in Otaniemi campus during my years here. I do not have enough space to thank all of them individually but I want to single out Nuutti Hyvönen for providing like-minded company.

As the people who know me well are no doubt aware of, research has not been my whole life during the thesis work. That is why I would like to thank all my friends in

Finland as well as the members of the NordForsk Nordic network of low-dimensional physics for numerous fun occasions during the past years. Lastly and most importantly, I would like to thank my sister Jaana, brother-in-law Kalle, nephew Aaro and parents Marjukka and Osmo for their invaluable support.

Otaniemi, October 2007

Teemu Ojanen

Contents

List of Publications

This thesis consists of an overview and of the following publications which are referred to in the text by their Roman numerals.

I O-P Saira, V. Bergholm, T. Ojanen, and M. Möttönen, *Equivalent qubit dynamics under classical and quantum noise*, Physical Review A **75**, 012308 (2007).

II Teemu Ojanen and Tero T. Heikkilä, *Quantum transition induced by the third cumulant of current fluctuations*, Physical Review B **73**, 020501(R) (2006).

III Tero T. Heikkilä and Teemu Ojanen, *Quantum detectors for the third cumulant of current fluctuations*, Physical Review B **75**, 035335 (2007).

IV T. Ojanen and T. T. Heikkilä, *State-dependent impedance of a strongly-coupled oscillator-qubit system*, Physical Review B **72**, 054502 (2005).

V T. Ojanen, A. O. Niskanen, Y. Nakamura, and A. A. Abdumalikov Jr, *Global relaxation in superconducting qubits*, Physical Review B **76**, 100505(R) (2007).

VI Teemu Ojanen and Janne Salo, *Possible scheme for on-chip element for squeezed microwave generation*, Physical Review B **75**, 184508 (2007).

VII Teemu Ojanen and Tero T. Heikkilä, *Photon heat transport in low-dimensional nanostructures*, Physical Review B **76**, 073414 (2007).

Author's contribution

I have carried out all the Thesis work reported here in Low Temperature Laboratory of Helsinki University of Technology, Finland. Most of the projects were motivated by the experimental developments in my home institute and abroad. In publications II, IV, VI and VII I have contributed to the central ideas and the formulation of the problems. I have also performed a majority of calculations and prepared the manuscripts for the most parts. In paper I I have contributed to the sections dealing with quantum noise and the Lindblad equation. I have written a part of the manuscript and contributed in its preparation in all stages. In paper V I have formulated the initial idea, calculated the analytical results and written the general theory part which forms roughly a half of the manuscript. In paper III I have contributed to the central ideas and given advice concerning the manuscript.

1 Introduction

Mesoscopic physics studies systems which are small on everyday scale, yet containing a large number of degrees of freedom. This relatively new field began to take shape in the early 80's as a combined result of improved experimental techniques and attempts to resolve to what degree macroscopic systems may exhibit quantum-mechanical behavior. Quantum mechanics is the most successful achievement of the 20th century science and its impact on our society and everyday life is difficult to overestimate. The theoretical formalism of quantum mechanics has been known in its current form for a long time, however, its paradoxes and broader implications remain far from clear. The gap between mathematical formulation and the physical world is not completely filled. Today, one of the most fascinating frontiers to study consequences of quantum laws is mesoscopic physics where the micro and macroworlds meet. In many applications, such as nanoscale electric circuits, mesoscopic systems allow high level of control in designing and manipulating them and many system parameters are typically tunable. This is in contrast to microscopic systems where structures are fixed and parameters are given by fundamental constants. Besides purely scientific interests, mesoscopic physics promises opportunities for a wide variety of technological and industrial applications in the future. Another motivation to study mesoscopic physics is the fact that quantum mechanics imposes fundamental restrictions to small devices that need to be taken into account in continuing miniaturization of structures.

Physics of open quantum systems has experienced a strong revival due to the interest towards mesosocopic systems. It is necessary to formulate quantum mechanics in a way that accommodates the influence of environment [1]. The open system formulation also offers new aspects to the quantum measurement problem, emphasizing the significance of the environment monitoring at the expense of a conscious observer [2]. Quantum measurement theory has also received a more concrete attention initiated by studies of electric fluctuations in nanostructures [3]. This Thesis is devoted to

the study of systems that are large compared to dimensions of individual atoms and molecules, and as such, usually very sensitive to environmental effects. Therefore all systems under study must be considered as open quantum systems interacting with their environments. As a concrete example we explore transitions effects caused by electric fluctuations in small quantum electronic devices. The topic is closely related to electron transport in nanostructures, quantum measurement theory and shielding of quantum electronics from harmful environmental effects. Another major topic of this Thesis is mesoscopic electron-photon systems that are currently under active study. These systems serve as test benches for quantum laws as well as promise variety of future quantum information and nanoelectronics applications [4]. Underlying similarity in open systems is the fact that the temporal evolution of systems is no longer governed by the unitary evolution of the Schrödinger equation which needs to be replaced by more general master equations leading to irreversible dynamics. Interactions between subsystems and their environment create correlations and, in case of large environments, information of correlations is carried away from the system permanently. From the point of view of subsystems, this leads to an irreversible behavior and typically to reduction of quantum superpositions.

1.1 Organization of this Thesis

In Chapter 2 I introduce concepts and machinery used in the theoretical treatment of open quantum systems and illustrate the formal side of the topic. In Chapter 3 I discuss the effects of non-Gaussian current fluctuations on probe quantum systems. The topic illustrates the dual interest in open system dynamics. On one hand, as is painfully clear in quantum information applications, noise coming from the environment contaminates the unitary temporal evolution of a subsystem and destroys its coherence properties. On the other hand, from the point of view of quantum measurement theory, an entangled subsystem can be used as a probe to extract information from its environment. In Chapter 4 I explore mesoscopic systems where

electron-photon interactions play an important role and introduce some quantum information applications. There I also discuss transport phenomena, forming an important subclass of open system problems where the focus is on the interplay between different parts of a system. Chapter 5 summarizes the overview and contains a brief outlook on the future developments in the field.

2 Dynamics of open quantum systems

The basic object used to represent a state of an open quantum system is a density operator $\hat{\rho}$. It contains the complete information of a quantum state at a given moment of time. A density operator is a Hermitian, positive operator $\langle n|\hat{\rho}|n\rangle \geq 0$ (with an arbitrary state $\langle n|$) with unit trace $\mathrm{Tr}(\hat{\rho}) = 1$. Diagonal matrix elements give probabilities for finding the system in corresponding states after a measurement, while off-diagonals contain information about quantum-mechanical phase coherence. In general, quantum-mechanical states represented by a density operator $\hat{\rho}$ can be classified into pure states which can be represented by state vectors and satisfy $\mathrm{Tr}(\hat{\rho}^2) = 1$, and mixed states which exhibit reduced phase coherence and fulfill $\mathrm{Tr}(\hat{\rho}^2) < 1$. Open systems are characterized by the fact that they generally are in mixed states. In absence of environmental effects the Schrödinger equation for a state vector is replaced by the von Neumann equation [5]

$$\frac{d\hat{\rho}(t)}{dt} = -\frac{i}{\hbar}\left[H, \hat{\rho}\right]. \tag{2.1}$$

The von Neumann equation describes a unitary temporal evolution of a general quantum state but it cannot be used to handle complicated systems efficiently. For this reason it is necessary to consider master equations which reduce the complicated dynamics to a feasible form. Expectation values of observables can be calculated from the density operator as $\langle \hat{A}(t)\rangle = \mathrm{Tr}(\hat{A}\hat{\rho}(t))$. Additional information can be found by studying multi-time correlations of the form $\langle \hat{A}_1(t_1)\hat{A}_2(t_2)\ldots\hat{A}_n(t_n)\rangle$ which cannot be obtained directly from $\hat{\rho}(t)$.

2.1 Tracing out environment; Master equations

A closed system is an idealization which, strictly speaking, is not realized in any physical system apart, perhaps, from the whole universe. Usually physical systems are imbedded in larger systems that act as environments. A fundamental problem

is to solve the reduced dynamics of a subsystem of interest. This can be achieved by solving the full dynamics of a system and its environment and projecting out the uninteresting part. Formally this is implemented by the Nakajima-Zwanzig equation [6, 7], which is generally difficult to solve. Thus it is necessary to devise methods that concentrate on the reduced system, allowing the environment effects to be taken into account without solving the full dynamics. This procedure, often referred to as tracing or integrating out environment degrees of freedom, leads to master equations that differ from Eq. (2.1) crucially by generating an irreversible temporal evolution. Irreversibilities manifest in energy dissipation and loss of coherence. There are several different approaches to open quantum dynamics their respective superiority depending on specific applications. The most direct way to derive the reduced dynamics is to start from the von Neumann equation and develop a perturbation expansion in the system-environment coupling term. A simple perturbative treatment can be improved by resummation techniques allowing formally exact manipulations in close analogy to many-body field theory. In Feynman-Vernon theory the reduced dynamics is formulated in terms of path integrals and environment effects are implemented by integration over influence functionals [1]. The Lindblad theory provides a general mathematical structure of the master equations yielding solutions satisfying a dynamical semi-group property [8, 9]. A complementary approach is provided by quantum Langevin equations in which the reduced system dynamics is formulated for operators in the Heisenberg picture [10, 11]. In this section the perturbation treatment follows the formulation of Refs. [12, 13].

Derivation of master equations usually requires writing the Hamiltonian of the total system in three contributions $H = H_{\rm s} + H_{\rm env} + H_{\rm int}$, where the first two terms correspond to the system of interest and its environment while the third term describes an interaction between them. A formal solution to the von Neumann equation (2.1) for the density operator of the total system can be written as $\hat{\rho}(t) = U(t,t_0)\hat{\rho}(t_0)U^\dagger(t,t_0)$ with $U(t,t_0) = e^{-\frac{i}{\hbar}H(t-t_0)}$. In the interaction picture

with respect to $H_{\rm int}$ the relation reads

$$\hat{\rho}^I(t) = U_I(t,t_0)\hat{\rho}(t_0)U_I^\dagger(t,t_0) \tag{2.2}$$

where $U_I(t,t_0) = Te^{-\frac{i}{\hbar}\int_{t_0}^t dt' H_{\rm int}^I(t')}$, $H_{\rm int}^I(t) = e^{\frac{i}{\hbar}(H_{\rm s}+H_{\rm env})t}H_{\rm int}e^{-\frac{i}{\hbar}(H_{\rm s}+H_{\rm env})t}$ and T is a time ordering operator. Assuming that the initial state of the total system is separable, $\hat{\rho}(t_0) = \hat{\rho}_{\rm s}^0 \otimes \hat{\rho}_{\rm env}^0$, the reduced density matrix $\rho_{\rm s}(n,m,t) \equiv \langle n|{\rm Tr}_{\rm env}\left[\hat{\rho}(t)\right]|m\rangle = \langle n,t|{\rm Tr}_{\rm env}\left[\hat{\rho}^I(t)\right]|m,t\rangle$ may be written as

$$\rho_{\rm s}(n,m;t) = \sum_{j,k}\Pi(n,m,t;j,k,t_0)\rho_{\rm s}^0(j,k), \tag{2.3}$$

where the propagator is given by

$$\Pi(n,m,t;j,k,t') = {\rm Tr}_{\rm env}\left[\hat{\rho}_{\rm env}^0\langle k,t'|\widetilde{T}e^{\frac{i}{\hbar}\int_{t'}^t d\bar{t}H_{\rm int}^I(\bar{t})}|m,t\rangle\langle n,t|Te^{-\frac{i}{\hbar}\int_{t'}^t d\bar{t}H_{\rm int}^I(\bar{t})}|j,t'\rangle\right], \tag{2.4}$$

and the trace is calculated over a complete set of environment states. In a graphical description the density matrix evolution is represented by two horizontal lines corresponding to the forward and backward propagation in time, see Fig. 2.1. The propagator can be expanded in powers of the operator $H_{\rm int}$ which is represented by a dot in propagation lines. The dots are connected by interaction lines which represent the trace over the environment and couple the forward and backward propagation lines. In the spirit of field-theoretic resummation of a many-body perturbation theory [14], one can derive the Dyson equation

$$\begin{aligned}\Pi(n,m,t;j,k,t') &= \Pi^0(n,m,t;j,k,t')+ \\ &+\int_{t'}^t dt_2\int_{t'}^{t_2}dt_1\Pi(n,m,t;r,s,t_2)\Sigma(r,s,t_2;p,q,t_1)\Pi^0(p,q,t_1;j,k,t'),\end{aligned} \tag{2.5}$$

where the repeated indices are summed. The self-energy $\Sigma(r,s,t_2;p,q,t_1)$ is defined as the sum of diagrams for which any vertical cut intersects at least one interaction line and $\Pi^0(n,m,t;j,k,t')$ is the propagator in the absence of the environment. In the eigenbasis of $H_{\rm s}$ it can be expressed as $\Pi^0(n,m,t;j,k,t') = \exp\left[-i(E_n-E_m)(t-t')/\hbar\right]\delta_{n,j}\delta_{m,k}$, where E_j are eigenvalues of $H_{\rm s}$. The Dyson equation (2.5) for the propagator is equivalent to a Bloch-type density operator

evolution

$$\frac{d\hat{\rho}_{\rm s}(t)}{dt} = -\frac{i}{\hbar}\left[H_{\rm s}, \hat{\rho}_{\rm s}(t)\right] + \int_{t_0}^{t} dt' \Sigma(t,t')\hat{\rho}_{\rm s}(t'), \tag{2.6}$$

where $\Sigma(t,t')$ is a superoperator with matrix elements $\Sigma(r,s,t;p,q,t')$. The diagram expansion can also be employed to calculate correlation functions such as $\langle \hat{B}(t_2)\hat{A}(t_1)\rangle$. The operators are placed on the closed time path (the Keldysh contour) depending on their ordering and dressed with all possible interaction processes [12], see Fig. 2.1.

The advantage of the above presented formalism is that it leads to an intuitive graphical representation of the perturbation theory on the Keldysh contour analogous to that of many-body Green's functions theory [15]. An obvious drawback is that the method is applicable only for initial states that are of a tensor product form in a system-environment space. This can be remedied by standard adiabatic switching techniques requiring additional work. A more subtle issue is the positivity of the density operator since perturbation expansions do not necessarily sustain the positivity and it can be violated after certain time [16]. This problem does not arise within the Born-Markov approximation [8], where the system-environment coupling is calculated in the lowest order and the self-energy is approximated as a local quantity in time. Physically the Born-Markov approximation is valid when the system and environment are weakly coupled and the decay of correlations in the environment is much faster than the reduced systems dynamics.

2.2 Lindblad evolution equation

The main application of reduced-system equations of motion, i.e. master equations, is to implement environment-induced relaxation and decoherence effects not taken into account by unitary dynamics of a closed system. The possible forms of master equations are strongly restricted by the requirements for density operators, particularly the positivity. In case of Markovian evolution the general form

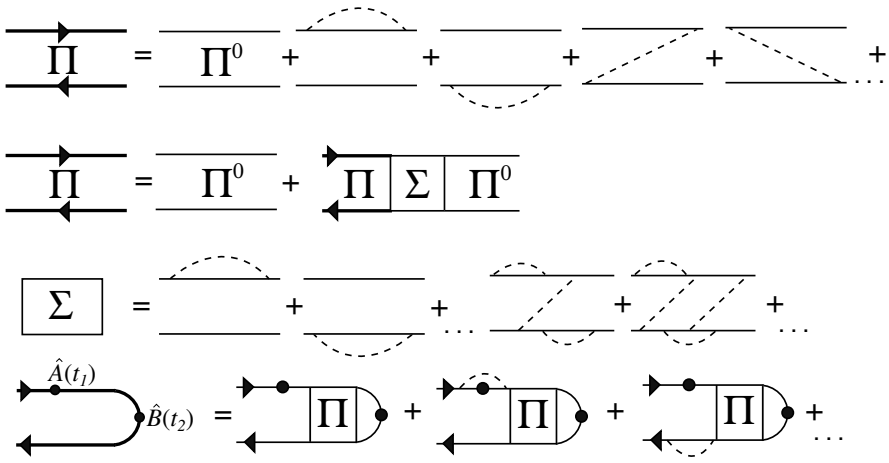

Figure 2.1: Diagrammatic perturbation expansion for the propagator Π. The propagator is obtained as a sum of all different diagrams and obeys the Dyson equation which is written in terms of the irreducible self-energy Σ. The lowest line represents the diagrammatic expansion of correlation function $\langle \hat{B}(t_2)\hat{A}(t_1)\rangle$.

of master equations is provided by the Lindblad equation [17]. Suppose that the reduced dynamics is given by a dynamical map $\rho \to \rho(t) = V(t)\rho(0)$, so that $\rho(t)$ is a density operator. Assuming that the dynamical map satisfies a semigroup property $V(t_1 + t_2) = V(t_1)V(t_2)$ for $t_1, t_2 \geq 0$, the temporal evolution is given by the Lindblad equation

$$\frac{d\hat{\rho}_{\rm s}}{dt} = -\frac{i}{\hbar}\left[H_{\rm s}, \hat{\rho}_{\rm s}\right] + \sum_i \gamma_i \left(2A_i\hat{\rho}_{\rm s}A_i^\dagger - A_i^\dagger A_i\hat{\rho}_{\rm s} - \hat{\rho}_{\rm s}A_i^\dagger A_i\right), \tag{2.7}$$

where γ_i are positive real numbers and A_i are so-called Lindblad operators acting in the reduced Hilbert space. In applications quantities γ_i usually correspond to excitation, decay and dephasing rates. The Lindblad equation (2.7) is the most general equation of motion satisfying the dynamical semigroup property [8, 9]. In physical applications, the Born-Markov approximation for the system-environment interaction often leads to a master equation of form (2.7) with case-specific Lindblad operators. Typically annihilation and creation operators play the role of Lindbad operators. The Lindblad equation provides a straightforward starting point in analyzing physics in the Markovian approximation and is well-behaving in numerical calculations. However, non-Markovian phenomena generally cannot be addressed.

2.3 Classical fluctuating potential as effective environment

Open quantum system dynamics is affected by environment degrees of freedom. Sometimes environment effects can be effectively described by a time-dependent stochastic term in the unitary von Neumann equation, as in Paper I. One could qualitatively study effects of a fluctuating bath of particles or external control parameters such as gate voltages and bias currents by introducing a stochastic term coupled to the system of interest. The philosophy of this approach is simple, though mathematically it is difficult to justify. It is by no means guaranteed that certain microscopic degrees of freedom can be identified as a fluctuating random potential. A single trajectory of the system experiencing the random potential corresponds to unitary evolution but an average over all potential realizations can generate nonunitary effects analogous to tracing out degrees of freedom. The random potential description reduces the Hilbert space dimension of the problem at the expense of the ensemble averaging.

In Paper I the dynamics of a closed system is studied under discrete classical Markovian noise. The noise is characterized by N different states having probabilities $P_k(t)$ which evolve in time according to

$$\partial_t P_k(t) = \sum_{j=1}^{N} \gamma_{kj} P_j(t) \tag{2.8}$$

and satisfy $\sum_{k=1}^{N} P_k(t) = 1$. Ensemble averaged temporal evolution is formulated in terms of conditional density operators $\rho_k(t)$ which represent the system in a noise state k, normalized so that $\mathrm{Tr}\,[\rho_k(t)] = P_k(t)$. The total density operator is obtained as

$$\rho(t) = \sum_{k=1}^{N} \rho_k(t) \tag{2.9}$$

satisfying the ordinary normalization. For each noise state there is a corresponding Hamiltonian H_k, so the evolution of $\rho_k(t)$ is given by

$$\partial_t \rho_k(t) = \frac{1}{i\hbar}\,[H_k, \rho_k(t)] + \sum_{j=1}^{N} \gamma_{kj} \rho_j(t), \tag{2.10}$$

where the second term corresponds to the random transitions between noise states. The system evolution is obtained as a solution to Eq. (2.10). For example, evolution of a quantum system experiencing Random Telegraph Noise (RTN) is obtained by solving the pair of equations

$$\partial_t \rho_\pm = \frac{1}{i\hbar}\left[H_\pm, \rho_\pm\right] \pm \frac{1}{\tau}(\rho_- - \rho_+), \tag{2.11}$$

where τ is the flipping rate between the two noise states. Equation (2.11) was used to study evolution of a two-level system under RTN in Paper I. It was also shown that the effective RTN description corresponds to a quantum-mechanical model where the two-level system is coupled to another two-level system subjected to an environment-induced relaxation. The connection between a random classical potential and the quantum model provides a physical motivation for using the RTN model. A similar version of Eq. (2.11) was employed in Ref. [18] to study the macroscopic quantum tunneling in a Josephson junction in the case of a fluctuating potential barrier.

2.4 Indirect quantum measurement

A measurement process of a quantum-mechanical system is formulated with a separate measurement postulate: a measurement of an observable $\hat{R} = \sum_m r_m |m\rangle\langle m|$ yields a result r_m with a probability $\mathrm{Tr}(|m\rangle\langle m|\hat{\rho}) = \rho_{mm}$. This formulation of a measurement process, though not fitting in the picture of the unitary quantum evolution and only partially understood, has proved indispensable in practice. Besides the ideal projective measurement, sometimes it is advantageous or necessary to consider an indirect measurement, where the system of interest is accessed through an additional quantum probe which is eventually subjected to the projective measurement. The indirect measurement is implemented by the Hamiltonian $H(t) = H_\mathrm{s} + H_\mathrm{p} + H_\mathrm{sp}(t)$ consisting of contributions from the system, the probe and the mutual interaction. Preferably $H_\mathrm{sp}(t)$ can be turned on at a given moment not to perturb the system before the measurement. Assuming that the probe is prepared at $t = 0$ to a known state $\hat{\rho}^0_\mathrm{p}$, the total initial density operator is $\hat{\rho}^0 = \hat{\rho}^0_\mathrm{s} \otimes \hat{\rho}^0_\mathrm{p}$ and

the probability to obtain an outcome r_m of a probe observable at a time $t > 0$ is

$$P_m = \mathrm{Tr}\left[|m\rangle\langle m|\hat{\rho}(t)\right] = \mathrm{Tr}\left[|m\rangle\langle m|U(t,0)\hat{\rho}_{\mathrm{s}}^0 \otimes \hat{\rho}_{\mathrm{p}}^0 U^\dagger(t,0)\right], \tag{2.12}$$

with $U(t,0) = Te^{-\frac{i}{\hbar}\int_0^t dt' H(t')}$. The quantum system and the probe entangle during the evolution, after which measurements of probe observables can be used to extract information about $\hat{\rho}_{\mathrm{s}}^0$. Depending on the nature of the system and the probe, two qualitatively different situations may arise. Suppose, for example, that the probe is a two-state quantum system coupled to another two-state system. Then the reduced density matrix of the probe characteristically exhibits periodic coherent oscillations. On the other hand, if the probe system is coupled to a large bath of particles, the reduced density matrix of the probe evolves eventually to a diagonal steady state determined by the bath coupling operator. Indirect measurement scheme is relevant in Chapter 3 in the context of detecting current fluctuations.

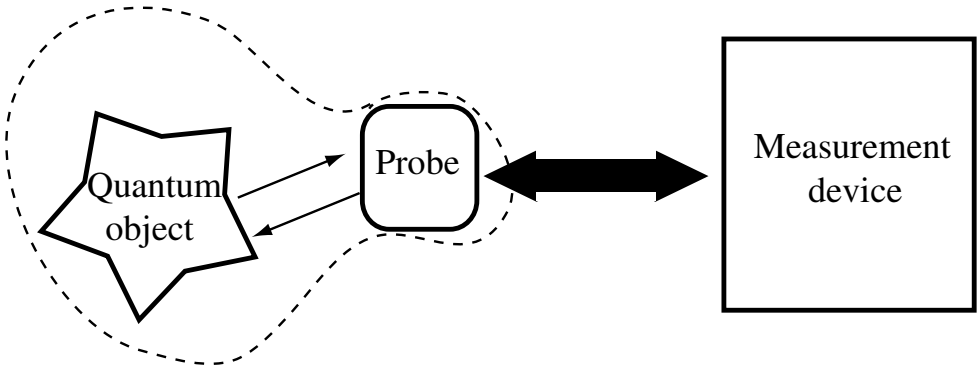

Figure 2.2: Schematic representation of indirect measurement. The quantum object entangles with the probe which is subsequently subjected to a projective measurement.

3 Characterization and detection of transitions induced by non-Gaussian current fluctuations

Measurable properties of many-body systems usually correspond to averaged values of many degrees of freedom. Average values provide restricted information and in a further analysis one is lead to study fluctuations about the mean. Fluctuations become more important as the system size is reduced, so they enter naturally in consideration in mesoscopic systems. Current fluctuations in nanostructures have been one of the central topics of mesoscopic physics for over a decade and exhibit interesting features that are absent in macroscopic conductors [19, 20]. This is because conduction electrons lose their quantum mechanical phase coherence in collisions with other electrons, phonons and dynamical impurities [21, 22]. Thus only in structures that are smaller or comparable to the electron phase relaxation length L_ϕ, which depends on temperature and microscopic details, quantum mechanical effects become important. The study of electric fluctuations experienced a significant stimulation from the theory of Full Counting Statistics (FCS) [3, 23] whose primary objective is to solve the electron number distribution in a transport process in a given interval of time. The essential result of FCS is that transmitted charge cumulants are obtained from the generating function $\mathcal{F}(\chi) = \ln \langle \widetilde{T} e^{-i\int dt \chi I(t)/2} T e^{-i\int dt \chi I(t)/2} \rangle$, where T ($\widetilde{T}$) denotes (anti)time ordering operator. Besides FCS, the statistics of fluctuations has been studied in many different contexts in various systems [24, 25, 26, 27, 28, 29].

Current fluctuations in mesoscopic structures consist of equilibrium Johnson-Nyquist noise described by the Fluctuation-Dissipation relation [30] and nonequilibrium shot noise caused by granularity of charge carriers [20]. Fluctuations provide information of the nature of a conduction mechanism and the intrinsic structure of the conductor that is not accessible from the average current. As a drawback, noise provides harmful influence on high-precision systems in the vicinity and needs to be taken into account in many applications. In this chapter we explore characterization of

transition effects induced by the third moment of current fluctuations in external quantum detector systems. Transition phenomena can be accessed through stationary probability distributions in contrast to the off-diagonal dynamics considered in detection of FCS. In the original FCS measurement scheme [3] the fluctuating current was coupled to a fictitious spin-$\frac{1}{2}$ system in vanishing magnetic field acting as a probe and the transmitted charge was identified as a rotation angle of the spin. Transition effects cannot be used for FCS measurement but are important in their own right and readily accessible. In some circumstances effects of noise even allow an effective temperature description. Much of the motivation of this chapter is provided by characterization of current fluctuations but the problem of a probe system coupled to a larger fluctuating environment is a very general one. The detection theory can be thought as a study of spontaneous emission and absorption in the presence of nonequilibrium environments. Detection aspects are discussed below in detail in context of two generic detector models, a two-level system and a harmonic oscillator.

3.1 Transitions induced by quantum noise

Consider the system schematically plotted in Fig. 3.1. The Hamiltonian of the system is

$$H = H_{\rm det} + H_{\rm env} + H_{\rm ecoup} + H_{\rm noise} + H_{\rm coup}, \tag{3.1}$$

where $H_{\rm det}$ corresponds to the detector system, $H_{\rm env}$ its environment and $H_{\rm noise}$ to the noise source. Remaining terms $H_{\rm ecoup}$ and $H_{\rm coup}$ describe the couplings of the detector system to the environment and the noise source, respectively. In the terminology of indirect measurement in Section 2.4, the noise source and environment correspond to the quantum object and the detector to the probe system. The detector part is assumed to have a discrete nondegenerate set of eigenstates $H_{\rm det}|n\rangle = E_n|n\rangle$ but the current source $H_{\rm noise}$ does not need to be specified in detail. The coupling is assumed to have a bilinear form $H_{\rm coup} = g\hat{I}\hat{B}$, where $\hat{I}$ is the current operator, $\hat{B}$ a

Hermitian operator acting in the detector Hilbert space and g a coupling constant. For simplicity, the average current effects are included to $H_{\rm det}$, so we may assume $\langle \hat{I} \rangle = 0$. The environment $H_{\rm env}$ and the coupling $H_{\rm ecoup}$ Hamiltonians implement a possible unideal behavior of the detector and are modeled by Caldeira-Leggett interaction [31, 32] $H_{\rm env} = \sum_j \hbar\omega_j \hat{a}_j^\dagger \hat{a}_j$, $H_{\rm ecoup} = \hat{A} \sum_j \lambda_j (\hat{a}_j + \hat{a}_j^\dagger) + \hat{A}^2 \sum_j \lambda_j^2 / \hbar\omega_j$.

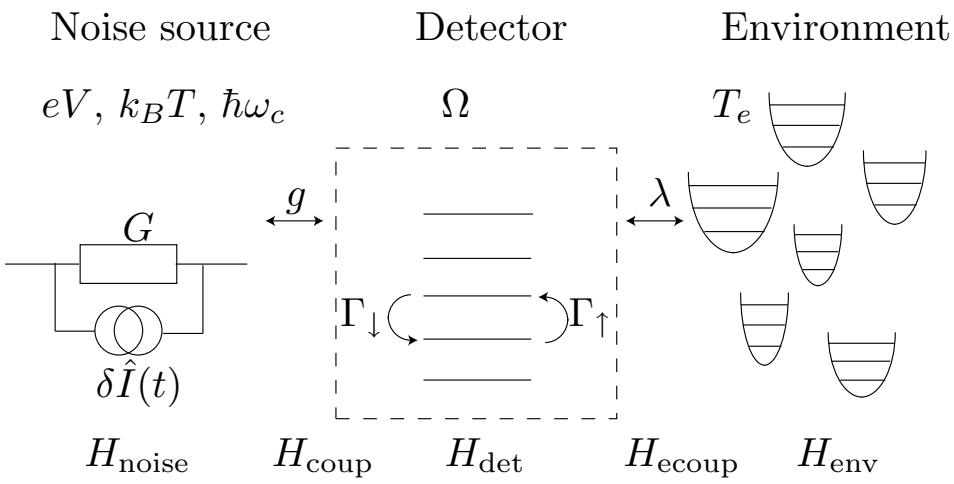

Figure 3.1: Generic scheme for noise measurement. The noise source is coupled to a detector system where it induces transitions. The detector is subsequently imbedded in a fluctuating environment independent of the measured noise source.

We are interested in the detector dynamics, so we study the reduced density operator $\hat{\rho}(t) = {\rm Tr}'\, \hat{\rho}_{\rm tot}(t)$ where $\hat{\rho}_{\rm tot}$ is the density operator for the whole system and the partial trace is calculated over the noise source and the environment. The transition rates can be obtained by solving the temporal evolution of a diagonal element of the reduced density matrix $\rho_{n'n'}(t) = \langle n'|\hat{\rho}(t)|n'\rangle$ with the initial condition $\rho_{n\,n}(t_0) = 1$ $(n \neq n')$. The transition rate $\Gamma_{n\to n'}$ is defined as the coefficient of the linearly increasing contribution to $\rho_{n'n'}(t)$ in the long-time limit. For calculating the rates the initial conditions are assumed to be of the product form $\hat{\rho}_{\rm tot}(t_0) = \hat{\rho}(t_0) \otimes \hat{\rho}_{\rm noise}(t_0) \otimes \hat{\rho}_{\rm env}(t_0)$, where $\hat{\rho}_{\rm noise}(t_0) \otimes \hat{\rho}_{\rm env}(t_0)$ describes the initial state of the noise source and the environment. In the following the rates are expressed in terms of the

noise power

$$S_I(\omega) \equiv \int_{-\infty}^{\infty} e^{i\omega(t-t_0)} \langle I(t) I(t_0) \rangle d\, t \tag{3.2}$$

and the partially time-ordered third cumulant

$$\delta^3 I(\omega_1, \omega_2) \equiv \int_{-\infty}^{\infty} d(t_1 - t_0) \int_{-\infty}^{\infty} d(t_2 - t_0) e^{i\omega_1 (t_1 - t_0) + i\omega_2 (t_2 - t_0)} \langle \widetilde{T}[I(t_0) I(t_1)] I(t_2) \rangle, \tag{3.3}$$

which emerge from the partial trace over the noise source. In the static case considered here, these correlators are independent of the time t_0. In Paper II it was for the first time recognized that the partially ordered correlator (3.3) plays an important role in transition phenomena. Previous literature was concentrating only on non-ordered or fully Keldysh symmetrized correlation functions arising from FCS. An essential lesson from the general considerations is that it is not a priori clear what type of correlation function contributes to the measured quantity. The current operators at different times do not commute and there is no universal form of correlation functions contributing to different observables. The relevant case-specific correlation function is determined by the observable of interest and the detailed measurement scheme. This problem is already present at the level of two-point correlation functions and it took a long time to recognize the emission-absorption interpretation arising from the different ordering of operators [33].

Up to the third order in couplings λ_j and g_i, the total transition rate is a sum of independent contributions arising from the noise source and environment $\Gamma_{m\to n} = \Gamma^{\mathrm{env}}_{m\to n} + \Gamma^{\mathrm{noise}}_{m\to n}$. The environment contribution

$$\Gamma^{\mathrm{env}}_{m\to n} = \frac{|A^{mn}|^2}{\hbar^2} 2\pi \sum_j \lambda_j^2 \left[\delta(\omega_{mn} - \omega_j)(n_j + 1) + \delta(\omega_{mn} + \omega_j) n_j\right] \tag{3.4}$$

gives the rate from state m to n due to a Gaussian bath, where we have introduced shorthands $A^{mn} = \langle m|\hat{A}|n\rangle$, $\omega_{mn} = (E_m - E_n)/\hbar$, $n_j = 1/(e^{\beta_e \hbar \omega_j} - 1)$ and $\beta_e = 1/k_{\mathrm{B}} T_e$ denotes the inverse bath temperature. Expression (3.4) can be evaluated further by introducing a continuous distribution of bath oscillators $f(\omega)$ and

replacing the summation by integration $\sum_j = \int_0^\infty d\omega f(\omega)$, yielding

$$\Gamma^{\rm env}_{m\to n} = \frac{|A^{mn}|^2}{\hbar^2} 2\pi \left[f(\omega_{mn})\lambda^2(\omega_{mn})(n(\omega_{mn})+1)\Theta(\omega_{mn}) \right.$$
$$\left. + f(-\omega_{mn})\lambda^2(-\omega_{mn})n(-\omega_{mn})\Theta(-\omega_{mn}) \right] = e^{\beta_e \hbar\omega_{mn}} \Gamma^{\rm env}_{n\to m}. \tag{3.5}$$

Tracing out the noise source up to the third order in the coupling constant g leads to expression

$$\Gamma^{\rm noise}_{m\to n} = \frac{1}{\hbar^2} g^2 |B^{mn}|^2 S_I(\omega_{mn}) + \Gamma^{(3)}_{m\to n}, \tag{3.6}$$

where

$$\Gamma^{(3)}_{m\to n} = \frac{g^3}{\hbar^3} {\rm Re} \sum_l \left[\int_{-\infty}^{\infty} \frac{\delta^3 I(\omega, \omega_{mn})}{\omega - \omega_{ln} - i\eta} d\omega B^{ml} B^{ln} B^{nm} \right]. \tag{3.7}$$

The first term on the right hand side of Eq. (3.6) is the well-known Golden Rule result which can be expressed in terms of frequency-dependent current noise [33]. The second term (3.7) was calculated in Paper II employing a diagrammatic method introduced in Chapter 2 and depends on the third-order correlator (3.3). Whereas the Golden Rule rate may give a finite contribution even in the case of equilibrium fluctuations, the expression Eq. (3.7) is non-vanishing only in nonequilibrium situations and characterizes effects of shot noise. The current operator $\hat{I}$ changes its sign in time-reversal transformation, so the three-point function vanishes in time-reversal invariant states.

3.2 Current correlators of point contacts

For calculating the populations of the detector states we need correlators (3.2) and (3.3). Finding them for a general mesoscopic conductor with interaction effects is a formidable task and only few results are known. However, in an important case of coherent transport through a quantum point contact with an energy-independent scattering matrix, the correlators can be found from the scattering theory [20, 34]. The noise power (3.2) can be written in the form $S_I(\omega) = S_I^Q(\omega) + S_I^{\rm exc}(\omega)$, where

the vacuum part is $S_I^Q(\omega) = 2\hbar\omega G\theta(\omega)$ and the excess noise is given by

$$S_I^{\rm exc}(\omega) = G\hbar\omega\left(\coth\left(\frac{\hbar\omega}{2kT}\right) - \mathrm{sgn}(\omega)\right) + F_2 G\frac{eV\sinh(\frac{eV}{kT}) - 2\hbar\omega\coth(\frac{\hbar\omega}{2kT})\sinh^2(\frac{eV}{2kT})}{\cosh(\frac{eV}{kT}) - \cosh(\frac{\hbar\omega}{kT})}$$
$$\stackrel{T\to 0}{\to} F_2 G(e|V| - \hbar|\omega|)\theta(e|V| - \hbar|\omega|). \qquad (3.8)$$

Here G is the point contact conductance, V is the applied voltage over it and $F_2 = \sum_n T_n(1-T_n)/\sum_n T_n$ is the Fano factor determined by the transmission eigenvalues T_n [33, 20]. Evaluation of $\delta^3 I(\omega_1, \omega_2)$ is more involved but can be carried out by using a technique developed in Ref. [34]. As was shown there, an arbitrarily ordered frequency-dependent current correlation function can be decomposed in terms of "in" $\hat{I}_{\rm in}$ and "out" $\hat{I}_{\rm out}$ current operator correlation functions. Using this formalism and notation of Ref. [34], the correlator (3.3) can be written as

$$\delta^3 I(\omega_1, \omega_2) = S_{ioo}(-\omega_1 - \omega_2, -\omega_2) + S_{ioo}(\omega_1, -\omega_2)$$
$$+ S_{ioo}(-\omega_2, -\omega_1 - \omega_2) - S_{ooo}(-\omega_1 - \omega_2, -\omega_2), \qquad (3.9)$$

where

$$S_{ioo}(\omega_1, \omega_2) = \int d(t_0 - t_1)\int d(t_1 - t_2) e^{i\omega_1(t_0 - t_1)} e^{i\omega_2(t_1 - t_2)} \langle \hat{I}_{\rm in}(t_0)\hat{I}_{\rm out}(t_1)\hat{I}_{\rm out}(t_2)\rangle$$

and analogously for S_{ooo}. The frequency dependence in Eqs. (3.8) and (3.9) arises only from Fermi distribution functions in the leads and does not reflect any features of a contact. These expressions are valid for frequencies much below the characteristic frequencies associated with internal dynamics or the collective response of structures such as charge pile-up. If the point contact is a part of an electric circuit with the impedance $Z_{\rm ext}(\omega)$ (see Fig. 3.2), fluctuations are modified in a frequency-dependent way. In steady-steady situations this can be taken into account by

$$S_I^c(\omega) = G(\omega)G(-\omega)S_I(\omega), \qquad \delta^3 I^c(\omega_1, \omega_2) = G(\omega_1)G(\omega_2)G(-\omega_1 - \omega_2)\delta^3 I(\omega_1, \omega_2),$$

where the factor $G(\omega) = 1/[1 + Z_{\rm ext}(\omega)G]$ accounts for the external circuit [20]. Now, in principle, we have all the necessary information for evaluating the probe system transition rates for point contacts.

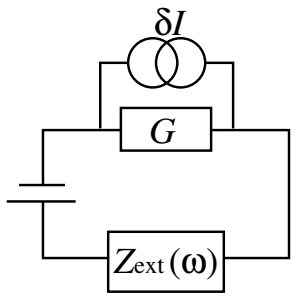

Figure 3.2: Quantum point contact G in series with an external circuit with impedance $Z_{\rm ext}(\omega)$.

3.3 Two-level and harmonic detectors

In the long-time evolution the detector density matrix $\rho_{nm}(t)$ typically tends to a diagonal steady-state form. The diagonal elements correspond to the probabilities $P_n \equiv \rho_{nn}$ to find the detector in states $|n\rangle\langle n|$. In a steady state, the probabilities of states connected by non-vanishing rates satisfy the detailed-balance condition $P_n/P_m = \Gamma_{m\to n}/\Gamma_{n\to m}$. If for all m, n the probabilities satisfy $P_n/P_m = \exp(\beta\hbar\omega_{mn})$ for some constant β, the probability distribution can be interpreted as a thermal distribution at an effective temperature $1/k_{\rm B}\beta$. Since the Golden-Rule contribution is a symmetric and the third-cumulant contribution (3.7) is an antisymmetric function of the current, the effective temperature is an asymmetric function of current in the case of a non-vanishing third moment.

The general Hamiltonian for a quantum two-level detector is

$$H_{TLS} = -\frac{B_z}{2}\sigma_z - \frac{B_x}{2}\sigma_x, \tag{3.10}$$

where $\sigma_{z/x}$ are Pauli matrices and $B_{z/x}$ are the effective magnetic fields that are often controllable in applications. We assume that the noise source is coupled to the detector according to

$$H_{\rm coup} = \frac{\hbar}{e} g\hat{I}\sigma_z.$$

and $\langle \hat{I} \rangle = 0$ because the average current effect can be absorbed to B_z. The ground and excited states of this system are given by $|0\rangle = -\beta|\uparrow\rangle + \alpha|\downarrow\rangle$ and $|1\rangle = \alpha|\uparrow\rangle + \beta|\downarrow\rangle$, with $\alpha = \cos(\phi/2)$, $\beta = \sin(\phi/2)$ and $\phi = \arctan(B_z/B_x)$. The energies of these states are $E_{0/1} = \mp\Omega/2$, $\Omega \equiv \sqrt{B_x^2 + B_z^2}$ and the relevant detector matrix elements are $\sigma_z^{11} = -\sigma_z^{00} = \cos(\phi)$ and $|\sigma_z^{01}|^2 = \sin^2(\phi)$. The Golden-Rule and third-moment rates can be written as

$$\Gamma_{0\to1}^{(2)} = \frac{g^2}{e^2}|\sigma_z^{01}|^2 S_{\rm noise}(-\Omega/\hbar), \tag{3.11}$$

and

$$\Gamma_{0\to1}^{(3)} = -\frac{g^3}{e^3}|\sigma_z^{01}|^2\cos(\phi){\rm Re}\left[\int_{-\infty}^{\infty} d\omega \frac{\delta^3 I(\omega,\Omega/\hbar)}{\omega+\Omega/\hbar-i\eta} - \int_{-\infty}^{\infty} d\omega \frac{\delta^3 I(\omega,\Omega/\hbar)}{\omega-i\eta}\right]. \tag{3.12}$$

The corresponding relaxation rates $\Gamma_{1\to0}^{(2/3)}$ can be obtained from the excitation rates with a substitution $\Omega \to -\Omega$. Importantly, if either B_z or B_x vanishes, the third moment contributions $\Gamma^{(3)}$ vanish also. This generic property follows from the structure of the product of detector matrix elements and is independent of noise. The explicit expressions for (3.12) was calculated analytically in various limits in Paper III. Assuming that the higher-order effects are insignificant, the effective temperature of the system can be defined as

$$k_B T_{\rm TLS} = \frac{\Omega}{\ln\left(\frac{\Gamma_{1\to0}^{(2)}+\Gamma_{1\to0}^{(3)}}{\Gamma_{0\to1}^{(2)}+\Gamma_{0\to1}^{(3)}}\right)}. \tag{3.13}$$

Important solid-state realizations of two-level quantum detectors are mesoscopic superconducting circuits, which have been used in characterization of noise [35].

A harmonic detector system is defined by the Hamiltonian

$$H_{\rm HO} = -\frac{\hbar}{2m}\partial_x^2 + \frac{1}{2}m\omega_0^2\hat{x}^2 = \hbar\omega_0\hat{b}^\dagger\hat{b}, \tag{3.14}$$

where $\hat{b}$ and $\hat{b}^\dagger$ are bosonic creation and annihilation operators. As a consequence of the general formula (3.7), if the fluctuating current couples linearly to the position or the momentum operator the rates $\Gamma_{m\to n}^{(3)}$ vanish. This is independent of the current noise and follows from the form of the matrix elements of the coupling

operators. This reasoning shows how harmonic systems are naturally robust against third moment transition effects and was used to justify the assumption of adiabatic nature of bias current fluctuations in a Josephson escape measurement [36]. If instead fluctuations modify the mass parameter of the oscillator, the resulting coupling term is of the form $H_{\mathrm{coup}} = -g\hat{I}(\hat{b}^\dagger - \hat{b})^2$. Non-vanishing contributions to transitions are $\Gamma^{(2)}_{n\to n+2}$, $\Gamma^{(2)}_{n+2\to n}$, $\Gamma^{(3)}_{n\to n+2}$ and $\Gamma^{(3)}_{n+2\to n}$, which all share the same n-dependence. This property, in the case when the Gaussian bath can be neglected, allows an effective temperature description according to

$$kT_{\mathrm{ho}} = \frac{2\hbar\omega_0}{\ln\left(\frac{\Gamma^{(2)}_{n+2\to n}+\Gamma^{(3)}_{n+2\to n}}{\Gamma^{(2)}_{n\to n+2}+\Gamma^{(3)}_{n\to n+2}}\right)}. \tag{3.15}$$

If the fluctuations couple to the square of the position instead of the momentum, the behavior remains qualitatively the same.

In summary, in this chapter we studied transition effects in simple quantum probe systems induced by nonequilibrium current fluctuations. The current operators at different times do not commute and generally specific combination contributing to the measured quantity depends on the details of the measurement scheme. The leading contribution to transition rates is proportional to the noise power (3.2) and the first correction to the third-moment correlator (3.3). The latter signals the nonequilibrium nature of the environment and vanishes in equilibrium. Apart from Section 3.2, the treatment is insensitive to the specific nature of the environment and thus very general.

4 Mesoscopic electron-photon systems

The theory of particles interacting with electromagnetic fields has a long and colorful history. One of the early triumphs of quantum theory was a successful explanation of spontaneous emission in excited atoms. Since then, interactions between light and matter have revealed a rich variety of phenomena from fantastically high to very low energies. Quantum electrodynamics and quantum optics are some of the best established theories of modern physics today. During the last decades developments in mesoscopic physics have opened an interesting possibility to engineer systems where the effects of electron-photon interactions are pronounced. With current technology the temporal evolution of solid-state quantum devices is routinely manipulated using external fields and radio-frequency signals. Recent advances have also enabled experimental studies of the strong coupling circuit cavity QED which has many advantages over the quantum optical counterpart. In circuit cavity QED a small electric circuit interacts with a single or multiple photon modes of a transmission line resonator [4, 37]. The phenomenon is interesting from the point of view of fundamental physics as well as numerous applications in quantum information processing, realizing single-photon sources and performing high-precision measurements. Besides controlled signals, photons also carry heat which propagates along electric circuits, a phenomenon which was experimentally measured recently [38]. At low temperatures photon radiation is an essential relaxation channel in metallic systems. A major advantage of mesoscopic electron-photon systems is the high-level control in designing and manipulating them.

In this chapter we study phenomena that are relevant in mesoscopic electron-photon systems. In the first section we consider a strongly coupled qubit-resonator system and explain how the oscillator response depends on the quantum state. The consequences of correlated relaxation of flux qubits is the topic of Section 4.2, where the proposed experimental scheme relies on methods of cavity QED. Section 4.3 concentrates on manipulation of quantum fluctuations in a SQUID circuit and applying

this to generate squeezed microwave radiation. Finally, Section 4.4 focuses on photon transport in a low-dimensional geometry and highlights an interplay between photon heat transport and electrical fluctuations.

4.1 Quantum impedance of a strongly coupled oscillator-qubit system

A harmonic oscillator coupled to a quantum two-level system is one of the generic systems appearing in many different physical contexts. The individual constituents are rare examples of exactly solvable systems and coupling them provides a qualitative explanation for a variety of phenomena. In quantum optics the system has been studied as a model of an atom interacting with a quantized electromagnetic cavity mode for decades. Oscillator-qubit systems have gained interest in solid-state physics after the experimental realization of circuit cavity QED in superconducting systems where small electric circuits are coupled to transmission line resonators [4, 37]. Circuit cavity QED applications is a fast growing field with promising prospects. Lately, the oscillator-qubit systems have been considered also in the context of mesoscopic electromechanical systems [39, 40]. In this section we consider a resonant oscillator-qubit system and study the response of the system under an external perturbation directed to the oscillator. The response depends on the quantum state of the system and the oscillator can be thought of as a probe in an indirect measurement of the qubit. Ideally this type of measurement could be used in probing the qubit properties and determining the state of the system. In case of electric circuits the response can be accessed by impedance measurements which have been realized in many experiments [4, 41, 42, 43, 44].

We describe the oscillator-qubit system with a variant of the Jaynes-Cummings Hamiltonian

$$H_{\mathrm{JC}} = \hbar\omega_0\,\hat{a}^\dagger\hat{a} - \frac{\hbar\omega_{\mathrm{qb}}}{2}\sigma_z + \frac{\hbar g}{2}\sigma_x(\hat{a}+\hat{a}^\dagger), \tag{4.1}$$

where ω_0 and $\omega_{\mathrm{qb}} \approx \omega_0$ correspond to the oscillator and qubit frequencies in res-

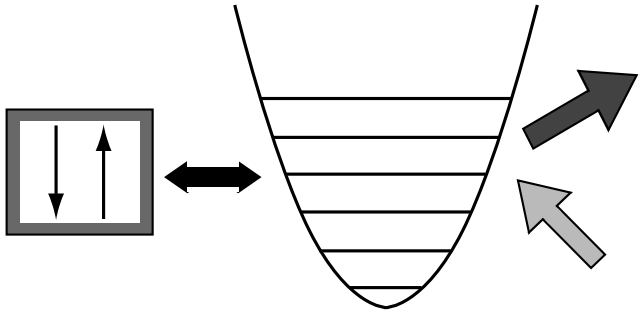

Figure 4.1: Two-state system coupled to a harmonic oscillator. Measurement of an oscillator response to an external perturbation can be used to extract information of the state of the system.

onance and g is their coupling strength. We concentrate on the strong-coupling regime where $g \sim 0.01\omega_0$. Since in practice both systems have dissipative losses, we introduce bosonic baths $H_B^{\rm qb} = \Sigma_i \hbar\omega_i \, \hat{b}_i^\dagger \hat{b}_i$ and $H_B^{\rm osc} = \Sigma_j \hbar\omega_j \, \hat{c}_i^\dagger \hat{c}_i$ to implement finite quality factors. The total Hamiltonian becomes

$$H = H_{\rm JC} + H_B^{\rm qb} + H_B^{\rm osc} + H_{\rm int}^{\rm qb} + H_{\rm int}^{\rm osc}, \tag{4.2}$$

where $H_{\rm int}^{\rm qb} = -\sigma_x \Sigma_i g_i (\hat{b}_i + \hat{b}_i^\dagger)$ and $H_{\rm int}^{\rm osc} = -(\hat{a}+\hat{a}^\dagger)\Sigma_j g_j' (\hat{c}_j + \hat{c}_j^\dagger)$ couple the system to the environment. Using LC resonator conventions, the canonical conjugate variables are written as

$$\hat{\phi} = \left(\frac{\hbar Z_b}{2}\right)^{\frac{1}{2}} (\hat{a} + \hat{a}^\dagger), \quad \hat{q} = i \left(\frac{\hbar}{2Z_b}\right)^{\frac{1}{2}} (\hat{a}^\dagger - \hat{a}), \tag{4.3}$$

where $Z_b = \sqrt{L/C}$, $\omega_0 = \sqrt{LC}$ and the operators satisfy $[\hat{\phi}, \hat{q}] = i\hbar$. The quantized LC resonator is an example of a quantum mechanical system of collective variables or a macroscopic quantum system, meaning that the canonical variables describe an ensemble of microscopic degrees of freedom. The oscillator response is obtained from susceptibility

$$\chi_q(\omega) = \frac{i}{\hbar} \int_0^\infty e^{i\omega t} \langle [\hat{q}(t), \hat{q}(0)] \rangle dt, \tag{4.4}$$

which measures the response of $\delta\langle \hat{q}(t) \rangle$ to a perturbation coupled to $\hat{q}$. Different response functions can be evaluated analogously by replacing the observables in the commutator in Eq. (4.4). The coupled system (4.1) can be diagonalized numerically

and the bath interaction can be taken into account perturbatively. The correlators in (4.4) were evaluated in Paper IV by employing the diagrammatic method outlined in Chapter 2.

The impedance of the resonator is related to the susceptibility by $Z(\omega) = i\omega\chi_q(\omega)$ and exhibits a strong dependence on the quantum state of the system. The positions of impedance peaks correspond to the excitation energies of the oscillator-qubit system and the linewidth reflects the dissipation, see Fig. 4.2. At finite temperature the resistance $\mathrm{Re}(Z(\omega))$ is positive and the relative hight of the peaks reflect the thermal population of states. The behavior is dramatically different in situations where the qubit is prepared in either of its eigenstates. When the qubit is prepared to the excited state the resistance exhibits negative peaks describing a net emission from the system due to the strong nonequilibrium nature of the state. It also illustrates how sensitive the system response is to the quantum state of the system. The impedance relaxes to its finite temperature value after a time corresponding to the spontaneous emission rate. As can be seen from Fig. 4.2 a), at low temperatures

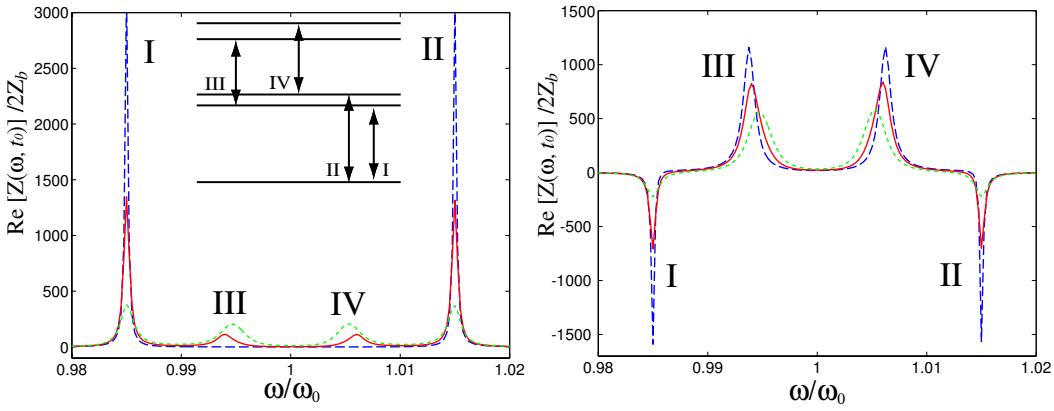

Figure 4.2: Real part of $Z(\omega, t_0)$ at temperatures $T = \hbar\omega_0/10k_\mathrm{b}$ (blue), $T = \hbar\omega_0/2k_\mathrm{b}$ (red) and $T = \hbar\omega_0/k_\mathrm{b}$ (green). The initial state at $t = t_0$ is prepared so that the oscillator is in the thermal state and the qubit state is up (the lower energy qubit state). Dissipation corresponds to a quality factor $Q = 10^4$ for a free oscillator. (b) Same as (a) but the initial state is prepared so that the qubit state is down.

$k_{\mathrm{B}}T \leq \hbar\omega_0$ the absorption spectrum exhibits peaks corresponding to transitions between the five lowest states that are approximately given by $|1\rangle = |0\rangle|\uparrow\rangle$, $|2\rangle = \frac{1}{\sqrt{2}}(|0\rangle|\downarrow\rangle - |1\rangle|\uparrow\rangle)$, $|3\rangle = \frac{1}{\sqrt{2}}(|0\rangle|\downarrow\rangle + |1\rangle|\uparrow\rangle)$, $|4\rangle = \frac{1}{\sqrt{2}}(|1\rangle|\downarrow\rangle - |2\rangle|\uparrow\rangle)$, $|5\rangle = \frac{1}{\sqrt{2}}(|1\rangle|\downarrow\rangle + |2\rangle|\uparrow\rangle)$. At higher temperatures more transitions come into play and eventually the individual peaks cannot be resolved [45]. In this section the analysis has been restricted to the case where the qubit and the resonator are tuned to resonance. However, for measuring the state of the qubit using the resonator as a probe it is optimal to work in the dispersive regime where the qubit and the resonator are detuned [4, 37]. Then the resonator absorption line is shifted depending on the state of the qubit. In Section 4.2 the measurement aspects are studied in more detail when we discuss a transmission measurement of Josephson flux qubits in a transmission line cavity.

4.2 Correlated relaxation of entangled qubits

In the last decade quantum information processing developed into an active branch of physics [46, 47]. Peter Shor's discovery of the powerful factorization algorithm [48] initiated tremendous efforts to realize a quantum computer operating on qubits. In order for a quantum computer to work, it is necessary for qubits to exhibit an adequate quantum-mechanical coherence to allow execution of algorithms. To achieve this, qubits must be well isolated from their environment to prevent decoherence. In this section we study dissipative environment effects by considering coupled qubits exposed to a global relaxation process. The global relaxation refers to the assumption that qubits are coupled to the same quantum bath. The global nature of the bath leads to remarkable features in spontaneous emission as first noticed by Dicke [49]. He showed that certain entangled states of noninteracting molecules decay more rapidly (superradiance) or are more stable than uncorrelated excitations (subradiance). The phenomenon was observed much later in the system of trapped nearby atoms [50] and has also been seen in quantum dot systems [51] where global phonon

modes play the role of the global bath.

As a concrete system we concentrate on Josephson flux qubits which consist of small superconducting loops interrupted by three Josephson junctions [52]. The two lowest energy levels corresponding to the oppositely circulating current states are well separated from the rest of the spectrum so at low temperatures the circuit can be thought of as an effective two-level system. Flux qubits are one of the most promising solid-state implementations for quantum bits exhibiting coherence times up to several microseconds. Energy relaxation has proved to be a serious limitation for further increase of their coherence time and therefore understanding it is of great importance. Unfortunately the origin and detailed mechanism of relaxation has remained largely unknown so far. By studying the decay of different two-qubit states one can determine whether the relaxation process is global, a feature that cannot be addressed in single-qubit experiments. In an experimental setting the measurement can be carried out by applying methods of cavity QED as discussed below. In addition, provided that the relaxation is caused by global fluctuations, one can construct long-lived entangled states.

The model we consider is determined by the Hamiltonian $H = H_q + H_{\rm env} + H_{\rm i}$, where

$$H_q = -\frac{\Delta}{2}\sum_i \sigma_z^{(i)} + J\sum_{i<j}\sigma_x^{(i)}\sigma_x^{(j)},\ H_{\rm i} = g\hat{x}\sum_i \sigma_x^{(i)}. \tag{4.5}$$

Here $\hat{x}$ is a Hermitian operator acting on the environment part of the Hilbert space. The many-body Hamiltonian of the environment $H_{\rm env}$ does not need to be specified in detail; its effects enter through correlation functions of $\hat{x}$. It is assumed that qubits have equal energy splittings Δ, interaction strengths J and bath coupling constants g. These features are realized in the case of similar qubits in close proximity to each other, compared to the relevant length scale of environment fluctuations. The form of the coupling in Eq. (4.5) is assumed to be $\sigma_x\otimes\sigma_x$-type as this is natural for optimally biased superconducting qubits. Also the σ_x-type coupling to the environment is natural since the effect of longitudinal coupling is strongly typically suppressed [53,

41]. In the case of two qubits the relevant Hilbert space is spanned by the vectors $|--\rangle \equiv |1\rangle, |-+\rangle \equiv |2\rangle, |+-\rangle \equiv |3\rangle, |++\rangle \equiv |4\rangle$. Supposing that $J \neq 0$, the system has four non-degenerate eigenstates $|d\rangle \equiv a|1\rangle + b|4\rangle$, $|\phi_s\rangle \equiv (|+-\rangle + |-+\rangle)/\sqrt{2}$, $|\phi_a\rangle \equiv (|+-\rangle - |-+\rangle)/\sqrt{2}$ and $|u\rangle \equiv -b|1\rangle + a|4\rangle$ with respective energies $-\sqrt{\Delta^2 + J^2}$, J, -J and $\sqrt{\Delta^2 + J^2}$. The coefficients are given by $a = ((1 + \Delta/2\sqrt{J^2 + \Delta^2}))^{1/2}$ and $b = -((1 - \Delta/2\sqrt{J^2 + \Delta^2}))^{1/2}$. The decay rates of the states can be calculated using the methods introduced in Chapter 2. In the lowest order in the bath coupling one obtains the Golden-Rule result

$$\Gamma_{\phi_s \to d} = \frac{g^2}{\hbar^2} 2(a+b)^2 S_x \left(\frac{\sqrt{\Delta^2 + J^2} + J}{\hbar} \right), \tag{4.6}$$

where $S_x(\omega) = \int_{-\infty}^{\infty} \langle \hat{x}(t)\hat{x}(0) \rangle e^{i\omega t} dt$. For the antisymmetric state the rate vanishes $\Gamma_{\phi_a \to d} = 0$, which is in striking contrast to Eq. (4.6). The stability of $|\phi_a\rangle$ is an exact consequence of the specific form of (4.5) and does not rely on the perturbation theory. Contrary to what was assumed in Eq. (4.5), the bath couplings of qubits never coincide exactly in experimental realizations. When qubits are realized artificially, for example, by quantum dots or superconducting circuits, individual Hamiltonians are not identical but depend on material parameters and sample-specific geometries. These features lead to deviations from the model (4.5) and modifies previous conclusions to some extent. As discussed in paper V, the scattering of parameters should not spoil the picture of the Dicke states supposing that the energies Δ_1, Δ_2 and the bath coupling constants g_1, g_2 of the two qubits satisfy $(\Delta_1 - \Delta_2)^2/J^2 \ll 1$ and $(g_1 - g_2)^2/(g_1 + g_2)^2 \ll 1$.

To study the nature of the relaxation process we suggest a system of two flux qubits [52, 54] with as identical parameters as possible coupled to a high-quality cavity [4], see Fig. 4.3. The lifetime of $|\phi_a\rangle$ should indeed be long even in the presence of imperfections — provided the assumption of globality of the noise holds. The qubit j (j=1,2) subspace when biased at the half-flux quantum point $\Phi_0/2$ consists of two circulating current states carrying a current of $\pm I_{\mathrm{p}}^j$. Tunneling between the states happens at a rate of $\Delta_j/\hbar$. Neglecting the off-resonant coupling to the cavity used

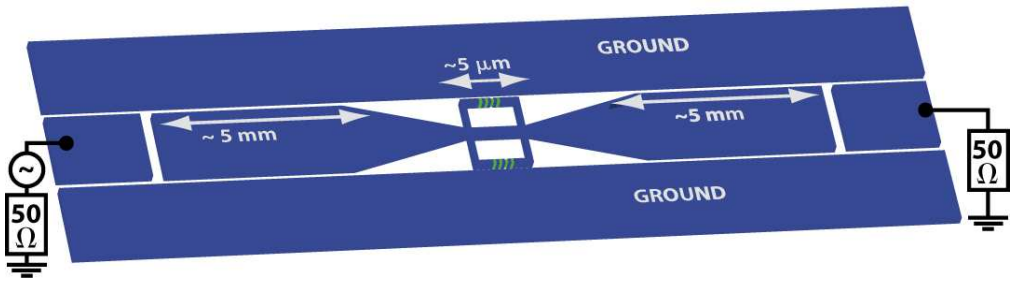

Figure 4.3: Schematic of the suggested experiment. The dimensions are exaggerated for clarity. The disconnected section in the middle forms a coplanar resonator whose resonant frequency is modified depending on the qubit state thus allowing for dispersive readout. The chirality is chosen such that the control microwave input via the same port as the readout couples antisymmetrically to the qubit.

for dispersive readout, the qubits are described by the Hamiltonian

$$H_q = -\sum_{j=1}^{2}\left(\frac{\Delta_j}{2}\sigma_z^{(j)} - \frac{\epsilon_j}{2}\sigma_x^{(j)}\right) + J\sigma_x^{(1)}\sigma_x^{(2)} \tag{4.7}$$

At the optimal point $\varepsilon_j = 2I_{\mathrm{p}}^j(\Phi - \Phi_0/2) = 0$ dephasing due to low-frequency flux fluctuations is minimized. To achieve symmetry and to optimize coherence we assume $\varepsilon_1 \approx \varepsilon_2 \approx 0$ and $\Delta_1 \approx \Delta_2$. As mentioned previously, the difference $|\Delta_2 - \Delta_1|$ should be small compared to $J = MI_{\mathrm{p}}^1 I_{\mathrm{p}}^2$ where M is the mutual inductance between the qubit loops. A realistic sample [55, 56] may have quite similar tunneling energies and a large coupling so as an example we assume $(\Delta_2 - \Delta_1)/h = 200$ MHz, $\Delta_1/h = 6$ GHz and $J/h = 1$ GHz. Choosing the bias of the second qubit to be $\varepsilon_2 = 0$ is easy using a global magnetic field and a typical e-beam patterned sample with nominally the same area may then have $\varepsilon_1/h = 200$ MHz [57]. These are conservative assumptions leading to the estimates

$$\Gamma_{\tilde{\phi}_s \to \tilde{d}} = 1.7 \times \frac{g^2}{\hbar^2} S_x(2\pi \times 7.2\,\mathrm{GHz}), \tag{4.8}$$

$$\Gamma_{\tilde{\phi}_a \to \tilde{d}} = 4.0 \times 10^{-3} \times \frac{g^2}{\hbar^2} S_x(2\pi \times 5.2\,\mathrm{GHz}), \tag{4.9}$$

for the transition rates. The factor $g^2/\hbar^2 S_x(\omega)$ in the above formulas is the characteristic relaxation rate for individual qubits and is typically of the order of 1 μs [53]. This translates into a 250 μs lifetime of the antisymmetric state under global

noise while the symmetric state decays in about 0.6 μs. Considering that presently energy relaxation is limiting coherence in flux qubits, spectacular coherence can be expected if a significant amount of the high-frequency noise is global.

The apparent complication in the present setting is on one hand the stability of $|\phi_a\rangle$ under any global high-frequency field and on the other hand the desire to excite the transition to study its decay. As shown in Fig. 4.3 we therefore assume that the qubits are coupled antisymmetrically (due to the left- and right-handed configurations of the qubits) to the center conductor such that a resonant drive via the transmission line can excite the $|d\rangle \leftrightarrow |\phi_a\rangle$ transition and ideally only that. That is, the microwave Hamiltonian can be approximated by $H_{\rm mw} = \alpha(t)(\sigma_x^{(2)} - \sigma_x^{(1)})$ for which clearly the excitation of $|\phi_a\rangle$ is possible since $\langle d|(\sigma_x^{(2)} - \sigma_x^{(1)})|\phi_a\rangle \neq 0$ but transitions between the symmetric states are forbidden. The antisymmetric microwave drive amplitude $\alpha(t)$ obeys $\alpha(t) = \delta\Phi(t)I_{\rm p}$ where $I_{\rm p}$ is the persistent current of the qubit and $\delta\Phi(t)$ is the ac flux drive. The state of the qubit can be detected from the shift of the cavity resonance frequency in a microwave transmission measurement in the same way as in Ref. [4], as discussed in detail in Paper V. Testing whether a significant part of the relaxation is due to global fluctuations amounts to measuring the lifetime of the state $|\phi_a\rangle$. Whether the result will be positive or negative is not known but in any case this should give valuable information about the origin of the noise and possibly enable a construction of long-lived entangled states.

4.3 Squeezed SQUID noise and microwave radiation

At the heart of the quantum theory lies the fundamental principle of describing observable quantities as Hermitian operators acting on quantum states. Generally these operators do not commute, a trait giving rise to the fundamental uncertainty principle first discovered by Heisenberg [58]. For non-commuting observables the statistical variations of their observed distributions, frequently called uncertainties,

cannot generally be arbitrarily small in a given state. However, the statistical variation of a single observable is not limited in any way by the uncertainty principle. The manipulation of uncertainties is referred to as squeezing. The squeezing of quantum fluctuations was first studied and experimentally verified in quantum optics, where the components of quantized electric field served as the squeezed observables [59]. Since then the phenomenon has been observed in superconducting circuits [60, 61], and more recently, there has been efforts to realize the squeezing in nanomechanical structures [62, 63, 64, 65]. Squeezing of quantum fluctuations is potentially interesting in future applications of quantum measurement. For example, nanomechanical resonators have been considered as realistic candidates in measuring ultra weak forces produced by gravitational waves [66]. Detection of effects of external forces is based on monitoring the position of a resonator which is blurred by quantum fluctuations. Reducing fluctuations through squeezing, it should be possible to detect smaller displacements and thus see perturbations due to gravitational waves.

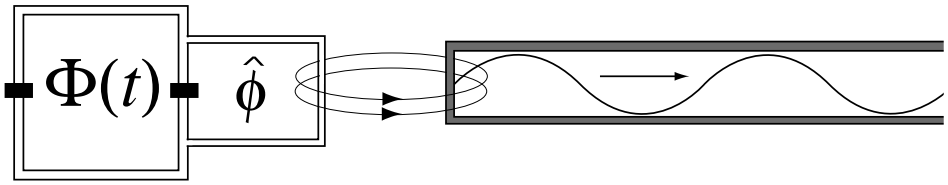

Figure 4.4: Resonantly driven SQUID loop inductively coupled to a transmission line. The black bars represent Josephson junctions and the physical quantities $\hat{\phi}$ and $\hat{Q}$ correspond to the magnetic flux through the right loop and the charge at the junctions. The (classical) flux $\Phi(t) \propto \sin(\omega_0 t)$ through the left loop is controlled by an external magnetic field.

In this section we consider squeezing of fluctuations in a flux-controlled Superconducting QUantum Interference Device (SQUID) circuit coupled to a transmission line (Fig. 4.4). In this application the SQUID is operated in a nearly harmonic regime, so the circuit can be thought of as an electromagnetic resonator. The squeezing mechanism is based on the parametric resonance, which is realized in harmonic systems where the characteristic angular frequency is subjected to a periodic perturbation $\omega^2 = \omega_0^2 + A\cos 2\omega_0 t$ [67]. In a quantum mechanical oscillator

this perturbation is known to cause a rapid oscillatory squeezing of the uncertainties [68]. Here the parametric resonance is realized by an external driving flux $\Phi(t)$ coupling through the Josephson term, squeezing SQUID fluctuations and feeding power to the system. This power is subsequently dissipated by microwave radiation. The Hamiltonian $H = H_S + H_{\rm TL} + H_{\rm int}$ consists of three contributions

$$H_S = \frac{\hat{Q}^2}{2C} + \frac{\hat{\phi}^2}{2L_S} - E_J \cos(\frac{2e\Phi(t)}{\hbar})\cos(\frac{2e\hat{\phi}}{\hbar}), \tag{4.10}$$

$$H_{\rm TL} = \sum_k \hbar\omega_k(\hat{c}_k^\dagger \hat{c}_k + 1/2), \qquad H_{\rm int} = M\frac{\phi}{L_S}\sum_k i\sqrt{\frac{\hbar\omega_k}{Ll}}(-\hat{c}_k + \hat{c}_k^\dagger), \tag{4.11}$$

where H_S, $H_{\rm TL}$ and $H_{\rm int}$ correspond to the SQUID [69], the transmission line and their interaction. The terms in Eq. (4.10) represent charging energy, magnetic energy and the Josephson interaction. The charge and the magnetic flux are conjugate variables satisfying $[\hat{\phi}, \hat{Q}] = i\hbar$. The parameter C is the capacitance of the junctions, L_S is the the loop inductance in the coupling loop and $\Phi(t)$ is the flux bias externally applied through the control loop.

The transmission line Hamiltonian and the magnetic interaction are determined by the eigenmodes ω_k, the capacitance and inductance per unit length c, l, the length L and the mutual inductance M. Assuming that the harmonic potential confines the flux $\hat{\phi}$ close to the origin, the SQUID Hamiltonian transforms to

$$H_S \approx \frac{\hat{Q}^2}{2C} + \frac{C\omega^2(t)}{2}\hat{\phi}^2, \qquad \omega^2(t) = \omega_0^2\left(1 + \frac{L_S}{L_J}\cos(\Phi(t)\,2e/\hbar)\right) \tag{4.12}$$

$$\tag{4.13}$$

with $\omega_0^2 = (L_S C)^{-1}$ and $L_J = \hbar^2/4e^2E_J$. From this form it is clear that the parametric resonance condition can be realized by the external drive $\Phi(t) = \hbar\omega_0 t/e$, which corresponds to a linearly increasing external bias. A linearly increasing flux is experimentally inconvenient and can be accurately replaced by an AC flux according to

$$\Phi(t) = (3/2\pi)\Phi_0 \sin(\omega_0 t), \tag{4.14}$$

as discussed in Paper VI. In the second quantization the SQUID Hamiltonian can be written as

$$H_S = \hbar\omega_0(\hat{a}^\dagger\hat{a} + \frac{1}{2}) + B\cos(2\,\omega_0 t)(\hat{a} + \hat{a}^\dagger)^2, \tag{4.15}$$

where $B = \hbar\omega_0 L/4L_J$ and $\hat{a}, \hat{a}^\dagger$ are canonical boson operators. Assuming that the interaction between the SQUID and the field can be treated in the Born-Markov approximation, the equation of motion for the reduced SQUID density operator is given by the Lindblad equation

$$\partial_t\hat{\rho} = -\frac{i}{\hbar}[H_S, \hat{\rho}] + \kappa(2\hat{a}\hat{\rho}\hat{a}^\dagger - \hat{a}^\dagger\hat{a}\hat{\rho} - \hat{\rho}\hat{a}^\dagger\hat{a}), \tag{4.16}$$

where the coefficient κ is related to the quality factor of the circuit by $\kappa = \omega_0/Q$. The value of κ can be estimated by $\kappa/\omega_0 = (M/L_S)^2 Z_0/Z_{\mathrm{TL}}$, where $Z_0 = \sqrt{L_S/C}$ and $Z_{\mathrm{TL}} = \sqrt{l/c}$. The coupled problem is then divided into solving the SQUID dynamics from (4.16) and working out the transmission line radiation. The voltage operator of the transmission line is of a typical radiation form

$$\hat{V}(x,t) = \hat{V}_0(x,t) + \frac{M\omega_0}{\pi L_S}\hat{\phi}(t - x/v), \tag{4.17}$$

where $\hat{V}_0(x,t)$ is the voltage operator in the absence of the SQUID loop, and the second term is proportional to the retarded SQUID field. Thus the properties of transmission line observables are inherited from the SQUID dynamics according to (4.17). This is analogous to how the emitted photon radiation from a coherent conductor reflects electronic shot noise [70].

The expectation values of operators $\hat{a}$, $\hat{a}^\dagger$, $\hat{a}^2$, $\hat{a}^{\dagger 2}$, and $\hat{a}^\dagger\hat{a}$ can be solved from the coupled set of differential equations of the form $\partial_t\langle\hat{a}\rangle = \mathrm{Tr}[\hat{a}\partial_t\hat{\rho}]$ etc. Numerical solution shows that for a strong drive, $B > \kappa$, the expectation values grow indefinitely in time, while for $\kappa > B$, the dissipation eventually compensates the resonant drive and the solutions are $2\omega_0$ periodic and bounded. In the limit $\kappa \to B + 0$, the lower limit of the periodic squeezing is about 0.75 times the vacuum value of $\Delta\phi \equiv \langle\hat{\phi}^2\rangle^{1/2}$ and $\Delta Q \equiv \langle\hat{Q}^2\rangle^{1/2}$ as depicted in Fig. 4.5. The squeezing of fluctuations can be

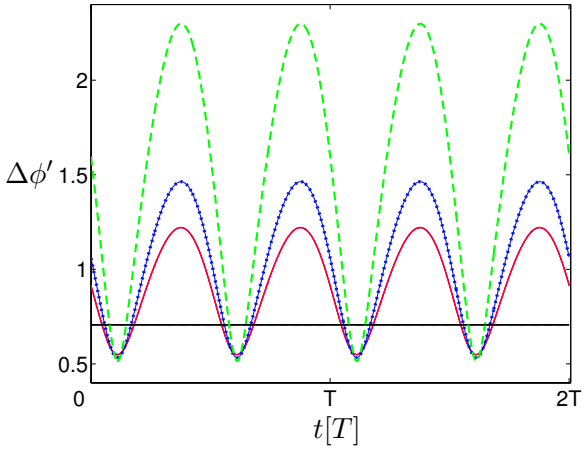

Figure 4.5: Uncertainty $\Delta\phi'$ of the bounded periodic solutions $\kappa = 1.5B$ (red, solid line), $\kappa = 1.3B$ (blue, dotted line) and $\kappa = 1.1B$ (green, with dashed line). The black horizontal dashed line marks the ground state value of $\Delta\phi'$. The lower envelope of the curves depicts the uncertainty of the reduced quadrature while the higher envelope corresponds to the increased quadrature of the rotating state. The minimum of the squeezing in the periodic solutions approaches a lower bound of about 0.75 times the ground-state value.

illustrated by the Wigner function

$$\rho_W(\phi', Q') = (2\pi)^{-1} \int_{-\infty}^{\infty} \langle \phi' - \frac{1}{2}y|\hat{\rho}|\phi' + \frac{1}{2}y\rangle e^{iQ'y}\, dy, \tag{4.18}$$

where we have defined dimensionless variables $\phi' = \phi/\sqrt{\hbar Z_0}$ and $Q' = Q/\sqrt{\hbar/Z_0}$. The circularly symmetric ground state of the SQUID is distorted to an ellipse by squeezing, see Fig. 4.6. For ideal squeezed states the principal axes of elliptical contour lines are inversely proportional to each other, reflecting the minimum uncertainty property $\Delta\phi'\Delta Q' = \frac{1}{2}$. As a consequence of dissipation, the distributions are broadened, which increases the uncertainty of quadratures $\Delta\phi'\Delta Q' > \frac{1}{2}$.

To calculate the SQUID and the transmission line noise one must find two-time correlation functions. This was done in Paper VI by applying the Quantum Regression formula [9]. According to the Regression formula, the function pair $\langle \hat{A}(t)\hat{a}(t')\rangle$ and $\langle \hat{A}(t)\hat{a}^\dagger(t')\rangle$ obey the same differential equations as $\langle \hat{a}(t')\rangle$ and $\langle \hat{a}^\dagger(t')\rangle$ for an arbitrary operator $\hat{A}(t)$. Choosing $\hat{A}(t) = \hat{a}^{(\dagger)}(t)$, one can calculate arbitrary two-time correlators and subsequently find transmission line properties such as

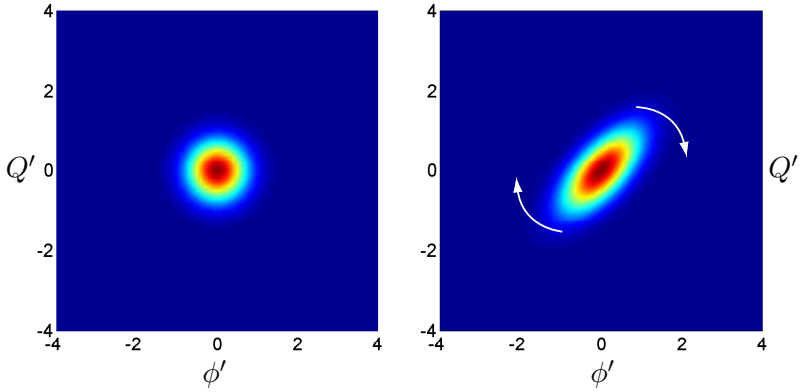

Figure 4.6: Wigner function of the ground state (left) and the periodic squeezed state $\kappa = 1.5B$ (right) in the (ϕ', Q')-plane. The squeezed state rotates clockwise as indicated by the arrows. The ellipse makes 2π rotation in time $T = 2\pi/\omega_0$.

$\langle \hat{V}(x,t)\hat{V}(x,t')\rangle$. The rapid rotation of the squeezing direction averages out the squeezing effects and the noise resembles that of the harmonic oscillator at finite temperature corresponding to the average energy of the system. Special detector schemes, such as resonantly rotating coupling, are required for direct verification of the squeezed noise spectrum. The studied SQUID circuit, when operated in the linear regime, is an electromagnetic counterpart of a mechanical resonator with similar prospects for applications. Thus, in analogy with measuring weak forces with mechanical resonators, the system could be considered in probing weak magnetic fields. Even though this is hypothetical at the moment, ultimately there is a need to manipulate quantum fluctuations in order to improve the accuracy of quantum-limited measurement devices in the future.

4.4 Photon heat transport in nanostructures

General physical arguments imply that a single-channel heat conductance has a universal upper limit $G_Q = \pi^2 k_B^2 T/3h$ irrespective of the precise nature of the heat carriers [71]. In particular, this remarkably universal feature is believed to hold

even for exotic quasiparticles obeying a fractional statistics. The single-channel heat transport has been experimentally measured for electrons [72], phonons [73] and quite recently for photons propagating in supeconducting leads between two metallic islands [38]. When electron heat conduction is restricted and the temperature is low enough for phonon modes to be frozen, the dominant method of thermal relaxation of metallic systems is photon transport [74]. In this section we study single-channel photon transport in nanostructures starting from a microscopic formulation. We introduce a model for photon exchange between a metallic island and a transmission line, explain the connection to electric fluctuations and discuss properties of the resulting radiation.

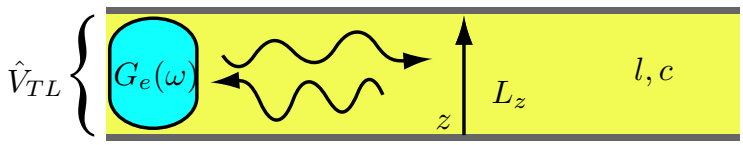

Figure 4.7: Metallic island coupled to the electromagnetic field of a transmission line. The voltage between the strips is $\hat{V}_{\rm TL}$.

Our starting point is a model consisting of a metallic island coupled to a parallel strip transmission line, see Fig. 4.7. The transmission line acts as a waveguide supporting a one-dimensional electromagnetic field. The total Hamiltonian of the system is $H = H_{\rm e} + H_\gamma + H_{{\rm e}-\gamma}$, where

$$H_{\rm e} = \int \hat{\Psi}^\dagger(r)\left(\frac{\hat{p}^2}{2m} + U(r)\right)\hat{\Psi}(r)dr + \frac{1}{2}\int \hat{\Psi}^\dagger(r)\hat{\Psi}^\dagger(r')V(r,r')\hat{\Psi}(r')\hat{\Psi}(r)drdr',$$
$$H_\gamma = \sum_j \hbar\omega_j(\hat{a}_j^\dagger\hat{a}_j + \frac{1}{2}) \qquad H_{{\rm e}-\gamma} = \frac{e}{L_z}\int \hat{\Psi}^\dagger(r)z\hat{\Psi}(r)dr\hat{V}_{\rm TL}. \tag{4.19}$$

The different terms correspond to the electron system, transmission line field and interaction between them. The electron number on the island is conserved, so the electric current between the transmission line and the island vanishes. In the following, a further specification of the electronic Hamiltonian H_e is irrelevant. The transmission line is characterized by its length L, distance between the parallel strips L_z, and inductance l and capacitance c per unit length. Operator $\hat{V}_{\rm TL} = \sum_j T_j(\hat{a}_j + \hat{a}_j^\dagger)$ is the

voltage operator at the end of the line. The field operators $\hat{\Psi}(r), \hat{\Psi}^\dagger(r)$ and creation and annihilation operators $\hat{a}_j, \hat{a}_j^\dagger$ satisfy canonical fermion and boson commutation relations. Constants $\omega_j = j\pi v/L$ (j is a positive integer) and $T_j = \sqrt{\hbar\omega_j/Lc}$ can be found by quantizing the line field [37]. The wave velocity v in the transmission line is given by $v = 1/\sqrt{lc}$.

The photon transport problem was solved in Paper VII by applying a nonequilibrium Green's function method [75]. The electron Hamiltonian does not commute with the total Hamiltonian, giving rise to an energy flow characterized by a current J_Q defined as

$$J_Q \equiv \langle \dot{H}_{\rm e} \rangle = -\frac{e}{mL_z} \left\langle \int \hat{\Psi}^\dagger(r) \hat{p}_z \hat{\Psi}(r) dr \hat{V}_{\rm TL} \right\rangle . \tag{4.20}$$

The notation $\langle \cdot \rangle$ stands for averaging over a density matrix of the total system. The focus is on the averages over nonequilibrium states where subsystems have a temperature gradient or the electron system is subjected to a finite voltage. The current (4.20) can be written as

$$J_Q(t) = -\frac{2e}{mL_z} {\rm Re} \sum_j T_j G_j^<(t,t), \qquad G_j^<(t,t') \equiv \langle \hat{P}(t) \hat{a}_j(t') \rangle, \tag{4.21}$$

where $\hat{P} = \int \hat{\Psi}^\dagger(r) \hat{p}_z \hat{\Psi}(r) dr$. The electric current perpendicular to the transmission line is related to the total momentum component by $\hat{I} = \frac{e}{mL_z}\hat{P}$. The transport problem is reduced to finding the "lesser" Green's function $G_j^<(t,t')$, which in a steady-state situation depends only on relative time $G_j^<(t,t') = G_j^<(t-t')$. Applying the equation-of-motion technique, the Fourier transform $G_j^<(\omega)$ can be expressed as

$$G_j^<(\omega) = -\frac{gL_z^2 m}{\hbar e^2} T_j \left[\frac{i}{\omega} \langle \hat{I}\hat{I} \rangle^r(\omega) D_j^<(\omega) + \frac{i}{\omega} \langle \hat{I}\hat{I} \rangle^<(\omega) D_j^a(\omega) \right], \tag{4.22}$$

where the superscripts ^{r}, ^{a} and $^<$ stand for "retarded", "advanced" and "lesser" and $D_j(\omega)$ denotes a free photon Green's function. At a finite temperature, the photon Green's functions are $D_j^<(\omega) = -2\pi i n_\gamma(\omega)\delta(\omega - \omega_j)$ and $D_j^a(\omega) = \frac{1}{\omega - \omega_j - i\eta} = \pi i \delta(\omega - \omega_j) + P\frac{1}{\omega - \omega_j}$, where P denotes principle value and $n_\gamma(\omega)$ is the Bose distribution. For a transmission line much longer than $\hbar\pi v/(k_B T)$, the sum over the field modes

can be replaced by integration according to $\sum_j = \frac{L}{\pi}\int_0^\infty dk = \frac{L}{\pi v}\int_0^\infty dw$ and the current takes the form

$$J_Q = 2Z_0 \int_0^\infty \frac{d\omega}{2\pi}\left[2\mathrm{Re}\langle\hat{I}\hat{I}\rangle^r(\omega)n_\gamma(\omega) - \langle\hat{I}\hat{I}\rangle^<(\omega)\right], \tag{4.23}$$

where $Z_0 = \sqrt{l/c}$ is the characteristic impedance of the transmission line. The correlators on the right hand side of Eq. (4.23) can be expressed in terms of the noise power $S_I = \int_{-\infty}^{\infty} e^{i\omega t}\langle\hat{I}(t)\hat{I}(0)\rangle dt$ as $\langle\hat{I}\hat{I}\rangle^<(\omega) = S_I(-\omega)$ and $\mathrm{Re}\langle\hat{I}\hat{I}\rangle^r(\omega) = \frac{1}{2}(S_I(\omega) - S_I(-\omega))$. Expression (4.23) is a formal solution in a sense that the current correlation functions depend on the external field. This makes it generally necessary to resort to approximations. The problem does not reduce to one-particle Green's functions which further complicates the treatment. However, the quadratic form of H_γ and the linear coupling term $H_{\mathrm{e-ph}}$, together with the density of states of a long transmission line is precisely a Caldeira-Leggett representation of an ohmic loss [31]. This notion microscopically motivates the circuit approximation, where the transmission line can be thought of as a resistor in series with the metallic island. Then the correlation functions in Eq. (4.23) can be approximated by

$$\langle\hat{I}\hat{I}\rangle(\omega) = \frac{\langle\hat{I}\hat{I}\rangle_e(\omega)}{|1 + G_e(\omega)Z_0|^2}, \tag{4.24}$$

where $\langle\hat{I}\hat{I}\rangle_e(\omega)$ and $G_e(\omega)$ are the current-current correlation function and conductance of the island in the absence of the electromagnetic field. Within the circuit approximation Eq. (4.23) transforms to

$$J_Q = \int_0^\infty \frac{d\omega}{2\pi}\frac{2Z_0}{|1 + G_e(\omega)Z_0|^2}\left[2\mathrm{Re}\langle\hat{I}\hat{I}\rangle_e^r(\omega)n_\gamma(\omega) - \langle\hat{I}\hat{I}\rangle_e^<(\omega)\right]. \tag{4.25}$$

Formula (4.25) provides a straightforward starting point in calculating photon transport properties.

A number of interesting results can derived from Eq. (4.25). In a quasiequilibrium situation, where the island and the field have an infinitesimal temperature gradient, the heat flow is given by

$$J_Q = \frac{4Z_0R_\mathrm{e}}{(R_\mathrm{e} + Z_0)^2}G_Q\Delta T, \tag{4.26}$$

where $R_\mathrm{e} \equiv 1/G_e$, $\Delta T = T_\gamma - T_e$ is a small temperature difference between electron and photon system and $G_Q = \pi^2 k_B^2 T/3h$ is the universal quantum of heat conductance [71]. This result verifies that the maximum heat conductivity is G_Q, achieved by a perfect matching $R_e = Z_0$. If the electron system is driven to a nonequilibrium state, the photon radiation is enhanced by electron shot noise. Supposing that the electron system can be described as a coherent conductor characterized by transmission eigenvalues T_m biased by an external voltage V, the energy current becomes

$$J_Q^\gamma = r\left[\frac{1}{2}G_0\mathcal{L}_0(T_\gamma^2 - T_\mathrm{e}^2) - \frac{1}{2}F_2 G V^2\right], \tag{4.27}$$

where $G_0 = e^2/h$, $G = G_0\sum_m T_m = 1/R_e$ is the island conductance, $F_2 = \sum_m T_m(1-T_m)/\sum_m T_m$ the Fano factor, $\mathcal{L}_0 = \pi^2 k_\mathrm{B}^2/3e^2$ the Lorenz number and $r = 4Z_0R_e/(Z_0+R_e)^2$. The last term in J_Q^γ corresponds to the increased emission by shot noise. Result (4.27) is valid for a system with energy-independent transmission eigenvalues described by current noise (3.8). As shown in Paper VII, using a more realistic form of the current noise the photon radiation enhancement displays features of the intrinsic properties of the conductor, see Fig. 4.8. The photon radiation leads also to a reduced Joule heating of the island as was discussed in Paper VII.

According to the analysis of this section, G_Q is the upper limit of heat conductivity in the studied model where the transmission line field couples only to current fluctuations perpendicular to the strips. However, if we introduce another transmission line with the same temperature but being perpendicular to the original one, the line couples to orthogonal current fluctuations and the maximum heat conductivity doubles to $2G_Q$ illustrating how the dimensionality plays an important role. This does not contradict the general statement that the maximum single-channel heat conductance is limited by G_Q because adding a perpendicular transmission line opens up a second independent transport channel, as discussed in Paper VII.

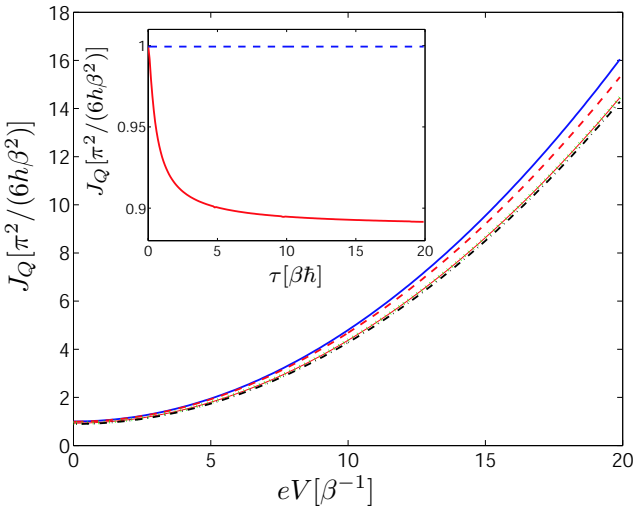

Figure 4.8: Energy flow from a symmetric chaotic cavity ($N_L = N_R = 1$) as a function of voltage. We assumed that the cavity conductance at zero frequency $G_e(0)$ is matched to Z_0^{-1}. The different curves correspond to different cavity charge relaxation times τ, $\tau = 0$ (solid), $\tau = 0.1\hbar\beta$ (dashed), $\tau = \hbar\beta$ (dotted), $\tau = 10\hbar\beta$ (dash-dotted). Inset shows the $\tau/\hbar\beta$-dependence of the heat flow from the cavity ($V = 0$), the horizontal dashed line corresponds to the heat flow from an ideally matched ohmic resistor without frequency dependence. When $\tau/\hbar\beta \ll 1$ the heat flow is close to the theoretical maximum and settles to a lower value as the fraction increases.

5 Conclusions

In this Overview we have discussed fluctuations and transport in mesoscopic systems where quantum mechanical effects play a key role. An underlying similarity in all the topics is the dynamical nature of considered phenomena and the necessity to resort to an open system description. The research contributions of this Thesis are motivated by recent experimental and theoretical studies in the field of mesoscopic physics and all the topics are also presently under an active study. A number of theoretical predictions were made in this Thesis work that could have relevance in future experiments. The most promising candidates for experimental verification are the transitions induced by the third moment of current fluctuations in quantum probes, the correlated decay and life time enhancement of entangled states in Josephson flux qubits, and the electron shot noise contribution to photon heat transport in nanostructures.

The characterization and detection of current fluctuations in mesoscopic structures was discussed in detail from the point of view of transition phenomena. Nonequilibrium current fluctuations generally have nonvanishing three-point current correlation functions which contributes to transition rates in external probe systems. The influence of current noise was considered on two generic probe models, a qubit and a harmonic oscillator. Current fluctuations play a dual role, on one hand they have a harmful influence in the vicinity of other systems. On the other hand fluctuations provide valuable information of the conducting system.

Mesoscopic electron-photon systems, a topic of a rapidly growing research field, can be designed and controlled accurately, allowing a number of interesting applications. We considered the response of a coupled qubit-resonator system to an external perturbation illustrating how it reflects the quantum state and properties of the system. Manipulation of quantum fluctuations was studied in an elementary SQUID circuit and applied to generation of squeezed microwave radiation. Propa-

gating photons carry energy, playing also an important role in thermal relaxation at low temperatures. We introduced a microscopic model for photon heat transport in nanostructures, considered the interplay between electric current fluctuations and photon heat transport.

Single-electron devices are routinely fabricated and used for many experimental purposes today. Lately, experimental advances is circuit cavity Quantum ElectroDynamics (QED) have allowed manipulation of single photons in nanoscale electromagnetic resonators. The next logical step, already in progress, is to construct electromechanical systems capable of manipulating single phonons in nanomechanical resonators. In the future one can hope to combine all these aspects in a single controllable system capable of single electron, photon and phonon manipulations. These systems could be used, perhaps, for creation and detection of single photons and phonons, and converting single phonons to photons and vice versa. Understanding of these composite systems requires efficient theoretical methods treating all the different particles on equal footing, possibly by generalizing the Landauer-Büttiker theory to accommodate the photon and phonon leads. Interesting future challenges in transport theory also include generalization of the known results of fluctuations and Full Counting Statistics to strongly correlated interacting systems. Transport theory of exotic particles of fractional charges in quantum Hall and Luttinger liquid structures offers many open questions. In solid state quantum information applications there are numerous obstacles in the way of constructing realistic quantum computers. No definite architecture allowing a sufficient coherence and control to execute quantum algorithms with an adequate number of qubits to solve practical problems has yet emerged. There remains a plenty of room for new proposals and improvement in physical realizations of qubits. Mesoscopic physics offers a great variety of interesting research topics in the future.

References

[1] R. P. Feynman and F. L. Vernon, Ann. Phys.(N.Y.) **24**, 118 (1963).

[2] W. H. Zurek, Phys. Today, October 1991 .

[3] L. S. Levitov, H. Lee, and G. B. Lesovik, J. Math. Phys **37**, 4845 (1996).

[4] A. Wallraff, D. I. Schuster, A. Blais, L. Frunzio, R.-S. Huang, J. Majer, S. Kumar, S. M. Girvin, and R. J. Schoelkopf, Nature (London) **431**, 162 (2004).

[5] J. von Neumann, *Die mathematischen Grundlagen der Quantenmechanik* (Springer-Verlag, Berlin, 1932).

[6] S. Nakajima, Progr. Theor. Phys. **20**, 948 (1958).

[7] R. Zwanzig, J. Chem. Phys. **33**, 1338 (1960).

[8] H. P. Breuer and F. Petruccione, *The Theory of Open Quantum Systems* (Oxford University Press, Oxford, 2002).

[9] H. J. Carmichael, *Statistical Methods in Quantum Optics 1: Master Equations and Fokker-Planck Equations* (Springer-Verlag, Berlin&Heidelberg, 1999).

[10] C. W. Gardiner, *Quantum Noise* (Springer-Verlag, Berlin&Heidelberg, 1991).

[11] C. Cohen-Tannoudji, J. Dupont-Roc, and G. Grynberg, *Atom-Photon Interactions* (Wiley, New York, 1992).

[12] H. Schoeller and G. Schön, Phys. Rev. B **50**, 18 436 (1994).

[13] J. Rammer, *Quantum Transport Theory* (Perseus Books, Reading, Massachusetts, 1998).

[14] G. D. Mahan, *Many-Particle Physics* (Springer, Berlin, 2000).

[15] J. Rammer and H. Smith, Rev. Mod. Phys. **58**, 323 (1986).

[16] S. M. Barnett and S. Stenholm, Phys. Rev. A **64**, 033808 (2001).

[17] G. Lindblad, Commun. Math. Phys. **40**, 119 (1976).

[18] J. Ankerhold and P. Pechukas, Europhys. Lett **52**, 264 (2000).

[19] C. W. J. Beenakker and C. Schönenberger, Phys. Today, May 2003 .

[20] Ya. M. Blanter and M. Büttiker, Phys. Rep. **336**, 1 (2000).

[21] S. Datta, *Electronic Transport in Mesoscopic Systems* (Cambridge University Press, Cambridge, 1995).

[22] E. Akkermans and G. Montambaux, *Mesoscopic Physics of Electrons and Photons* (Cambridge University Press, Cambridge, 2007).

[23] M. Kindermann and Yu. V. Nazarov, in *Quantum Noise*, edited by Yu. V. Nazarov and Ya. M. Blanter, vol. 97 of *NATO Science Series II* (Kluwer, Dordrecht, 2003).

[24] J. P. Pekola, T. E. Nieminen, M. Meschke, J. M. Kivioja, A. O. Niskanen, and J. J. Vartiainen, Phys. Rev. Lett. **95**, 197004 (2005).

[25] B. Reulet, J. Senzier, and D. Prober, Phys. Rev. Lett. **91**, 196601 (2003).

[26] T. T. Heikkilä, P. Virtanen, G. Johansson, and F. K. Wilhelm, Phys. Rev. Lett. **93**, 247005 (2004).

[27] R. K. Lindell, J. Delahaye, M. A. Sillanpää, T. T. Heikkilä, E. B. Sonin, and P. J. Hakonen, Phys. Rev. Lett. **93**, 197002 (2004).

[28] A. V. Galaktionov, D. S. Golubev, and A. D. Zaikin, Phys. Rev. B **68**, 235333 (2003).

[29] J. Tobiska and Yu. V. Nazarov, Phys. Rev. Lett. **93**, 106801 (2004).

[30] H. B. Callen and T. A. Welton, Phys. Rev. **83**, 34 (1951).

[31] A. J. Leggett, S. Chakravarty, A. T. Dorsey, M. P. A. Fisher, A. Garg, and W. Zwerger, Rev. Mod. Phys. **59**, 1 (1987).

[32] U. Weiss, *Quantum Dissipative Systems* (World Scientific Publishing, Singapore, 1999).

[33] R. Aguado and L. P. Kouwenhoven, Phys. Rev. Lett. **84**, 1986 (2000).

[34] J. Salo, F. W. J. Hekking, and J. P. Pekola, Phys. Rev. B **74**, 125427 (2006).

[35] O. Astafiev, Yu. A. Pashkin, Y. Nakamura, T. Yamamoto, and J. S. Tsai, Phys. Rev. Lett. **93**, 267007 (2004).

[36] A. V. Timofeev, M. Meschke, J. T. Peltonen, T. T. Heikkilä, and J. P. Pekola, Phys. Rev. Lett **98**, 207001 (2007).

[37] A. Blais, R.-S. Huang, A. Wallraff, S. M. Girvin, and R. J. Schoelkopf, Phys. Rev. A **69**, 062320 (2004).

[38] M. Meschke, W. Guichard, and J. P. Pekola, Nature (London) **444**, 187 (2006).

[39] A. D. Armour, M. P. Blencowe, and K. C. Schwab, Phys. Rev. Lett. **88**, 148301 (2002).

[40] E. K. Irish and K. Schwab, Phys. Rev. B **68**, 155311 (2003).

[41] A. Wallraff, D. I. Schuster, A. Blais, L. Frunzio, J. Majer, M. H. Devoret, S. M. Girvin, and R. J. Schoelkopf, Phys. Rev. Lett. **95**, 060501 (2005).

[42] M. A. Sillanpää, T. Lehtinen, A. Paila, Yu. Makhlin, L. Roschier, and P. J. Hakonen, Phys. Rev. Lett. **95**, 206806 (2005).

[43] M. A. Sillanpää, T. Lehtinen, A. Paila, Yu. Makhlin, L. Roschier, and P. J. Hakonen, Phys. Rev. Lett. **96**, 187002 (2006).

[44] T. Duty, G. Johansson, K. Bladh, D. Gunnarsson, C. Wilson, and P. Delsing, Phys. Rev. Lett. **95**, 206807 (2005).

[45] I. Rau, G. Johansson, and A. Shnirman, Phys. Rev. B **70**, 054521 (2004).

[46] M. A. Nielsen and I. L. Chuang, *Quantum Computation and Quantum Information* (Cambridge University Press, Gambridge, 2000).

[47] J. Gruska, *Quantum Computing* (McGraw-Hill, New York, 1999).

[48] P. W. Shor, in *35th Annual Symposium on Foundations of Computer Science* (IEEE Computer Society Press, Los Alamitos, CA, 1994).

[49] R. H. Dicke, Phys. Rev. **93**, 99 (1953).

[50] R. G. DeVoe and R. G. Brewer, Phys. Rev. Lett. **76**, 2049 (1996).

[51] T. Fujisawa, D. G. Augustin, Y. Tokura, Y. Hirayama, and S. Tarucha, Nature (London) **419**, 278 (2002).

[52] J. E. Mooij, T. P. Orlando, L. Levitov, L. Tian, C. H. van der Wal, and S. Lloyd, Science **285**, 1036 (1999).

[53] D. Vion, A. Assime, A. Cottet, P. Joyez, H. Pothier, C. Urbina, D. Esteve, and M. H. Devoret, Science **296**, 886 (2002).

[54] I. Chiorescu, Y. Nakamura, C. J. P. M. Harmans, and J. E. Mooij, Science **299**, 1869 (2003).

[55] T. Hime, P. A. Reichard, B. L. T. Plourde, T. L. Robertson, A. V. Ustinov C.-E. Wu, and J. Clarke, Science **314**, 1427 (2006).

[56] A. O. Niskanen, K. Harrabi, F. Yoshihara, Y. Nakamura, and J. S. Tsai, Phys. Rev. B **74**, 220503(R) (2006).

[57] A. O. Niskanen, private communication.

[58] W. Heisenberg, Zeitschrift für Physik **43**, 172 (1927).

[59] R. Loudon and P. L. Knight, J. Mod. Opt. **34**, 709 (1987).

[60] B. Yurke, P. G. Kaminsky, R. E. Miller, E. A. Whittaker, A. D. Smith, A. H. Silver, and R. W. Simon, Phys. Rev. Lett. **60**, 764 (1988).

[61] B. Yurke, L. R. Corruccini, P. G. Kaminsky, L. W. Rupp, A. D. Smith, A. H. Silver, R. W. Simon, and E. A. Whittaker, Phys. Rev. A **39**, 2516 (1989).

[62] M. P. Blencowe and M. N. Wybourne, Physica B **280**, 555 (2000).

[63] R. Ruskov, K. Schwab, and A. N. Korotkov, Phys. Rev. B **71**, 235407 (2005).

[64] K. C. Schwab and M. L. Roukes, Phys. Today, July 2005 .

[65] M. D. LaHaye, O. Buu, B. Camarota, and K. C. Schwab, Science **304**, 74 (2004).

[66] V. P. Braginsky and F. Ya. Khalili, *Quantum Measurement* (Cambridge University Press, Cambridge, 1992).

[67] L. D. Landau and E. M. Lifshitz, *Mechanics* (Pergamon Press, Oxford, 1976).

[68] I. Averbukh, B. Sherman, and G. Kurizki, Phys. Rev. A **50**, 5301 (1994).

[69] Yu. Makhlin, G. Schön, and A. Shnirman, Rev. Mod. Phys. **73**, 357 (1999).

[70] C. W. J. Beenakker and H. Schomerus, Phys. Rev. Lett. **86**, 700 (2000).

[71] J. B. Pendry, J. Phys. A: Math. Gen. **16**, 2161 (1983).

[72] O. Chiatti, J. T. Nicholls, Y. Y. Proskuryakov, N. Lumpkin, I. Farrer, and D. A. Ritchie, Phys. Rev. Lett. **97**, 056601 (2006).

[73] K. Schwab, E. A. Henriksen, J. M. Worlock, and M. L. Roukes, Nature (London) **404**, 974 (2000).

[74] D. R. Schmidt, R. J. Schoelkopf, and A. N. Cleland, Phys. Rev. Lett. **93**, 045901 (2004).

[75] H. Haug and A.-P. Jauho, *Quantum Kinetics in Transport and Optics of Semiconductors* (Springer-Verlag, Berlin&Heidelberg, 1996).